Rapport SGC 162

Design of energy systems for gas–heated through air dryers

Henrik Weineisen & Stig Stenström
INSTITUTIONEN FÖR KEMITEKNIK, LTH

Rapport SGC 162 • ISSN 1102-7371 • ISRN SGC-R--162-SE

SGC:s FÖRORD

FUD-projekt inom Svenskt Gastekniskt Center AB avrapporteras normalt i rapporter som är fritt tillgängliga för envar intresserad.

SGC svarar för utgivningen av rapporterna medan uppdragstagarna för respektive projekt eller rapportförfattarna svarar för rapporternas innehåll. Den som utnyttjar eventuella beskrivningar, resultat e dyl i rapporterna gör detta helt på eget ansvar. Delar av rapport får återges med angivande av källan.

En förteckning över hittills utgivna SGC-rapporter finns på SGC´s hemsida www.sgc.se.

Svenskt Gastekniskt Center AB (SGC) är ett samarbetsorgan för företag verksamma inom energigasområdet. Dess främsta uppgift är att samordna och effektivisera intressenternas insatser inom områdena forskning, utveckling och demonstration (FUD). SGC har följande delägare: Svenska Gasföreningen, E.ON Gas Sverige AB, E.ON Sverige AB, Lunds Energi AB, Göteborg Energi AB, och Öresundskraft AB.

Följande parter har gjort det möjligt att genomföra detta utvecklingsprojekt:

Statens Energimyndighet
Metso Paper Karlstad AB
SCA Hygiene Products AB

SVENSKT GASTEKNISKT CENTER AB

Jörgen Held

Introduction

The aim of this report is to summarize the work that has been done during the three years of the project “Design of energy distribution systems for gas-heated through air dryers”. The project has been funded by the Swedish Gas Centre, Metso Paper and the Center for Chemical Process Design and Control. The work has been performed by Henrik Weineien, who is employed as a Ph.D. student at the Department of Chemical Engineering, Lund University. At the end of the three years Henrik Weineisen has reached an academic level corresponding to the Swedish “licentiate degree”. Henrik has chosen to continue the work for two more years towards a Ph.D. degree

Main work and results

Summary

The aim of the work has been to acquire a better understanding for the through-drying process and to use this knowledge to improve the energy efficiency of the process. In order to learn more about the mechanisms involved in through-drying, the process has been studied by experiments and by mathematical modelling.

The work has been focused on the following areas:

A. Review of the existing literature on through-drying
B. Initial computer modelling of the through-drying process and comparison with experimental data from the literature
C. Study of the overall energy balances of the through-drying system
D. Experimental work with the aim of acquiring data at conditions comparable to industrial intensities (The work was performed at the Metso Paper research facility, Biddeford, Maine, USA.)
E. Modelling of through-drying at high intensity and comparison with experimental data (ongoing)

The project has resulted in the following journal publications, conference presentations and reports:

1. Weineisen, H. Through-drying of paper – a literature review, *report published at the department of Chemical Engineering, Lund University, 2003*
2. Weineisen, H. Modeling through-drying of tissue - effect of pore size distribution on drying characteristics, *Paper presented at the 14th International Drying Symposium, Sao Paulo, Brazil, August 2004*
3. Weineisen, H. Modeling through-drying of tissue - effect of pore size distribution on drying characteristics, *Drying Technology, 23(9-11), pp. 1909-1923*
4. Weineisen, H. Through-drying of tissue – an experimental study, *report published at the department of Chemical Engineering, Lund University, 2005*
5. Weineisen, H., Morrison, D., Parent L. and Stenström, S., Through-drying of tissue at high intensities- an experimental study, *submitted in March 2006 for publication in the Journal of Pulp and Paper Science*

6. Weineisen, H., Morrison, D., Parent L. and Stenström, S., Experimental study of Through-Drying of tissue at industrial conditions-drying results and flow analysis, *paper submitted to the 15th International Drying Symposium, Budapest, Hungary, August 2006*

A. Literature review (publication 1)

The initial literature review provided a good start of the project by studying what previous research on the subject had lead to and by identifying which areas were still not very well understood. The main finding was that experimental results for through-drying at conditions comparable to industrial conditions were missing in the literature. Industrial conditions are characterised by high drying air temperature and high airflow rates resulting in *average* drying rates as high as 550 kg/m^{2}h. In the previous studies the *maximum* drying rates had been in the range of 2-130 kg/m^2, with most of the studies closer to the lower side of this range. In industry the process is operated such that the pressure drop across the web is kept constant, i.e. the airflow rate increases as drying proceeds and the permeability increases. Despite this fact, previous work on through-drying has been focused on experiments at constant airflow rate.

B. Initial computer modelling (publications 2 and 3)

The results from this study showed the importance of including non-uniformity in terms of a pore size distribution to models of through-drying. It was shown that large pores dry out preferentially and then act as bypass channels for the drying air. Consequently, in through-drying of tissue, a large portion of the drying air possibly passes through the paper without any contribution to the evaporation rate. The results also showed that the early onset of the falling rate and absence of a constant rate period in through-drying at higher intensities may be the results of channelling effects and not due to inefficient local mass transfer rates.

Modelling through-drying by describing the heat or mass transfer by fundamental correlations, yields very high transfer coefficients which result in local saturation of the drying air even at high flow rates. Models that do not include the effect of a pore size distribution yield satisfying results at low intensity conditions, where saturation of the drying air is known to occur. At higher drying intensity, where the falling rates starts much earlier than for the low intensity experiments, a model that includes the effects of pore size distribution showed that even if local saturation of the drying air still occurs at the local level, channelling effects may be the reason for the drying air not reaching saturation during the falling rate period.

Figure 1 shows the simulation result for a model where the porous structure of the paper has been represented by a single mean diameter. The simulation agrees very well with the simulated data. Figure 2 shows the simulation results for the same model as in Figure 1 but compared to a case of higher intensity (In Figure 2 model 1 to 4 refers to different correlations for heat and mass transfer). Figure 2 shows that a model based on a single mean diameter is not suitable as the drying intensity is increased. Figure 3 shows the results for a model in which the porous structure is represented by a pore size distribution (23 pore sizes). It is clear that the channelling effects occurring as the larger pores dry out can explain the early onset of the falling rate period. This is further illustrated by Figure 4, where the moisture ratios of the areas associated with each pore size are plotted as a function of time. The model predicts a much more rapid increase in drying rate than the experiments (Figure 3). A possible reason for this is that the experiments were performed using wet pressed paper, while the model assumes that all pores are open to flow already at the beginning. However, in industry dewatering is performed by vacuum dewatering and it is expected that the initial increase in drying rate is more rapid than for the experiments shown here. Figure 4 shows the moisture ratio for the areas with different pore sizes and the average moisture ratio as a function of time. The pore sizes were in the range of 18 to 40 micrometers and the simulation shows great differences in drying times for the different areas.

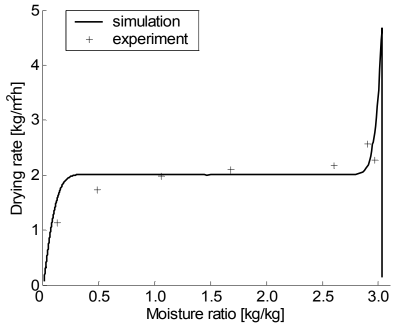

Figure 1. Predicted drying rate curve and experimental data for the low intensity case.

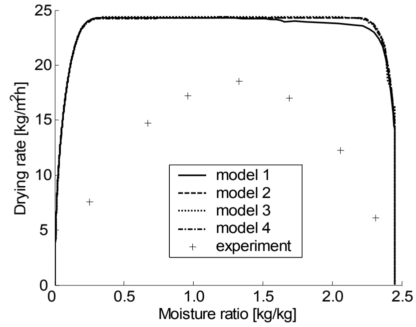

Figure 2. Predicted drying rate curve and experimental data for a case of higher intensity.

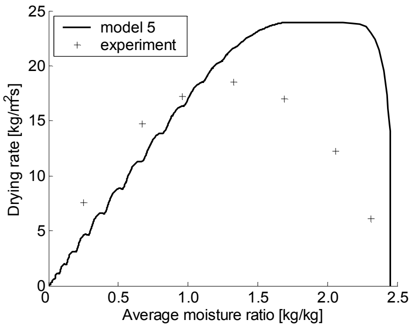

Figure 3. Predicted average drying for a normal distribution of 23 pore sizes.

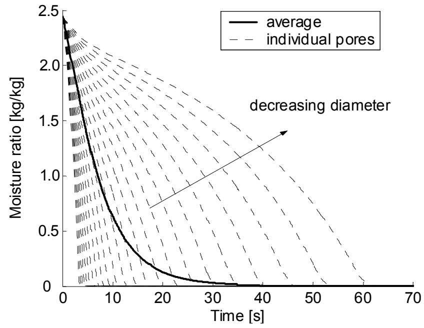

Figure 4. Moisture ratio as a function of drying time for areas with different pore sizes.

C. Overall energy balance

Figure 5 shows a schematic flow chart for a single through-drying unit. In the typical industrial application, two such units are operated in series followed by a conventional Yankee-dryer where the drying is completed.

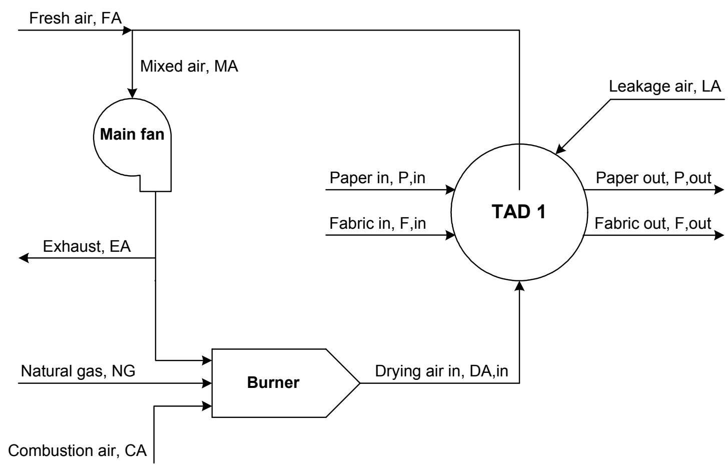

Figure 5. Schematic flow chart for one through drying unit

In the typical operating case, the dew point of the exhaust air is rather low, approximately 65-75 ºC, which of course limits the potential for heat recovery, especially in integrated mills where the pinch temperature, i.e. the temperature above which energy is needed, is approximately 120 ºC. In the present system, exhaust gases are simply discharged to the surroundings, without any heat recovery. Preheating of the combustion air by heat exchange with the exhaust gases have thus far been discarded, mainly because of the large and expensive heat exchangers needed for this operation.

In order to study the effect of different process configurations, a steady state model of the system was set up. The model was used to study the effect of preheating the combustion air based on typical machine data provided by Metso Paper.

The three following different configurations where evaluated:

1. Preheating the combustion air of dryer 1 by heat exchange with the exhaust stream from dryer 1
2. Preheating the combustion air of dryer 2 by heat exchange with the exhaust stream of dryer 2
3. Preheating the combustion air of dryer 1 by heat exchange with the exhaust stream of dryer 2

In order to estimate the heat exchanger area needed for a given preheat temperature, the heat transfer was assumed to take place in a counter current heat exchanger with a heat transfer coefficient of 35 $W/m^2\,ºC$. A function given by the computer program Icarus (used for techno-economical calculations) was used to estimate the cost of the heat exchanger needed. The cost given by this function includes all costs for installing the heat exchanger. The natural gas price was set to 0.23 SEK/kWh (65 SEK/GJ), which was the approximate cost for natural gas in Sweden at the time when the work was done. Figure 6 shows the savings on natural gas that can be expected for different preheat temperatures of the combustion air of the two through-dryers. The pay-back time as a function of preheat temperature for the three different cases is shown in Figure 7. The pack-back time is just a simple pay-back time, i.e. it does not include any interest rate. Cases 1 and 2, where the exhaust air streams from the two units are used to preheat their respective combustion air streams, show minimum pay-pack times of 3.9 and 5 years at preheat temperatures of approximately 90 and 130 ºC respectively. For these preheat temperatures, the corresponding natural gas usage is 3.8 and 6.6% lower than in the initial (base case) configuration.

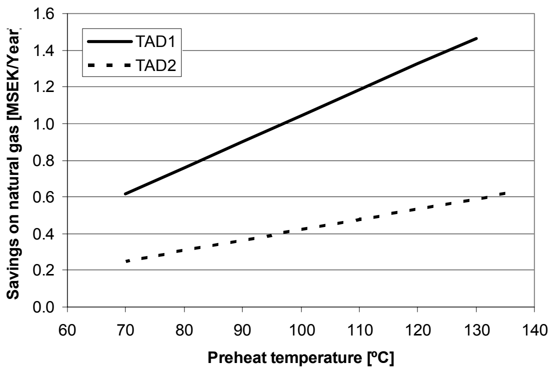

Figure 6. Savings on natural gas for dryer 1 and 2 by preheating the combustion air

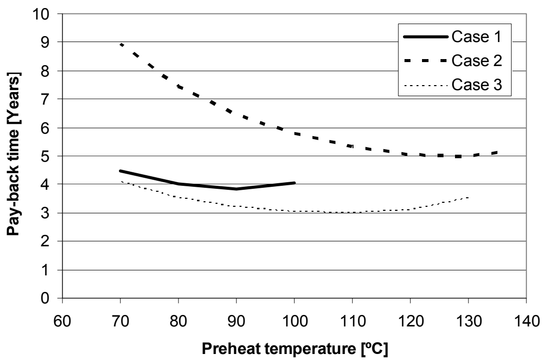

Figure 8. Pay-back time as function of the preheat temperature for the three cases

The third case, where the combustion air of dryer 1 is preheated by heat exchange with the exhaust stream of dryer 2, shows a minimal pay-back time of about 3 years at a preheat temperature of approximately 110 ºC. The gas usage of the first unit is lowered by 5.0% by applying this configuration. The shorter pay-back time of the third case is due to a combination of two factors, i.e. a relatively large logarithmic mean temperature difference (small heat exchanger) in combination with a relatively large amount of combustion air that is preheated (the air flow rate being higher in dryer 1).

The model was also used to study the effects of using the exhaust air from the second unit as combustion air for the first. The results, summarized in Table 1, show that the use of natural gas in the first unit may be reduced by 5.9% by applying the new configuration. The specific energy use is then decreased from 3.8 to 3.6 MJ/kg. Since moist air from the second unit is used as combustion air for the first unit, the exhaust and consequently the fresh air intake have to be increased, resulting in an 8.5% increase of the flow through the main fan. Furthermore, the exhaust temperature is lowered from 110 to 106 ºC and the moisture ratio of the exhaust air is lowered from 0.31 to 0.28 kg/kg as a consequence of the larger fresh air intake. Using relevant prices in SEK for electricity and natural gas, i.e. 0.3 SEK/kWh and 65 SEK/GJ, shows that the operating costs of the studied hypothetical machine may be reduced by 1.3 million SEK/year (approx. 180 000 US $/year). These calculations were based on a pressure difference over the fan of 0.69 kPa (as given by Metso Paper) and a fan efficiency of 0.7. It was further assumed that the machine runs 8000 hours per year.

Table 2. Comparison between the base case and the new configuration

Stream	Base case	New config.
Natural gas (kg/s)	0.272	0.256
Combustion air (kg/s)	6.74	8.00
Drying air in (kg/s)	49.7	49.7
Leakage air (kg/s)	6.90	6.90
Fresh air (kg/s)	0.70	5.59
Mixed air (kg/s)	58.0	62.2
Exhaust (kg/s)	14.0	20.2

D. Experimental study (publications 4, 5 and 6)

Experimental data for through-drying of tissue at intensities comparable to industrial conditions were obtained by the study. The study covered three basis weights, 20, 30 and 40 g/m^2, dried at drying air temperatures of 100, 150 and 200 ºC. Unlike most experimental data on through-drying in the literature, the experiments in the present study were performed under conditions of constant pressure drop across the sample, which is how the process is operated in industry. The study covered a total of eighteen different combinations of the variables basis weight, drying air temperature and pressure drop. Pressure drops in the range 1-5.2 kPa were studied depending on basis weight and the desired through-flow rate. The results from the 242 experiments show drying times ranging from approximately 0.6 to 3.5 seconds, at average drying rates ranging between approximately 100 and 300 kg/m2h. The experiments were performed using the laboratory equipment of Metso Paper at the company's research facility in Biddeford, Maine, USA.

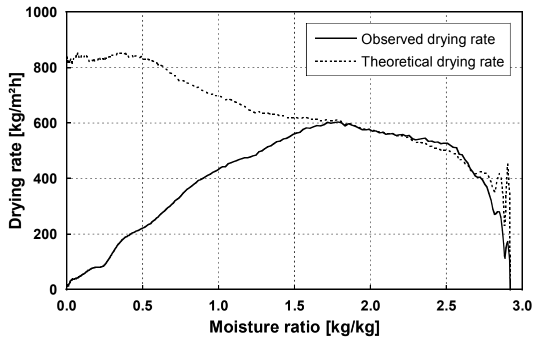

Figure 9. Observed and theoretical drying rate curves.

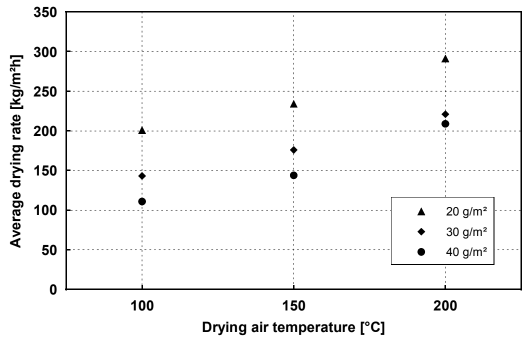

Figure 10. Average drying rates for different basis weights at different drying air temperatures. The pressure drop was 2.6 kPa.

In Figure 9 the drying rate curve for a typical sample is plotted together with a theoretical drying rate curve calculated as the drying rate resulting from adiabatic saturation of the drying air. The increase in theoretical drying rate with decreasing moisture ratio is the result of the increase in permeability, and thus the flow rate, as drying proceeds. The comparison shows that, after the rapid initial increase in drying rate, the observed drying rate coincides with the theoretical drying rate, before the drying rate reaches its maximum and the falling rate period begins. The period during which the observed drying rate coincides with the theoretical drying rate is controlled by two factors: the air flow rate and drying air saturation. Therefore, this period in the constant pressure drop experiments corresponds to the constant drying rate period of constant flow rate experiments.

Figure 10 shows the average drying rate for the different basis weights dried at a pressure drop of 2.6 kPa and drying air temperatures 100, 150 and 200 °C. As can be seen in Figure 10, as the drying air temperature is increased from 100 to 200 °C the average drying rate increases by 50 to 100%, depending on basis weight.

In publication 6, the experimental data was used to analyse the flow characteristics for flow through paper.

E. Modelling of through-drying at high intensity (ongoing work)

The work is now focused on dynamic modelling of through-drying at industrial conditions, i.e. drying at a high constant pressure drop across the web and high drying air temperature. The results will be compared to the experimental work described above and the aim is to, based on this model, develop a dynamic model for a complete through-drying machine. This model will then be used to study the possibilities of new process configurations for reducing the natural gas use and making the process more competitive.

Through Drying of Tissue
- An Experimental Study

Henrik Weineisen
Department of Chemical Engineering,
Faculty of Engineering, Lund University

LUTKDH/(TKKA-7003)/1-17/(2005)

Acknowledgements

First I would like to thank Larry Parent, former manager of Process Technology and Development at Metso Paper, Biddeford, Main, USA, for giving me the opportunity to come and work in his laboratory.

I would also like to use this opportunity to express my gratitude to David Morrison, process and development engineer at Metso Paper, Biddeford, Maine, USA, without whose invaluable help and sharp analyses considering the equipment this study would never have come together within in reasonable time.

Finally, I would like to thank SGC (Swedish Gas Center) for the grant that made this study possible by funding my travel costs and accommodation.

Abstract

Experimental data for through drying of tissue paper at intensities comparing to industrial conditions are presented. The study covers three basis weights, 20, 30 and 40 g/m^2. Each basis weight was dried at drying air temperatures 100, 150 and 200 ºC. Unlike most experiments on through drying described in the literature, the experiments in this study were performed under such conditions that the pressure drop across the sheet was kept constant, which is also the case in industrial applications. Pressure drops were in range 1-5 kPa, depending on basis weight and on desired average through-flow rate. For each basis weight, experiments were performed at two different pressure drops. As a result, the study covers a total of eighteen different combinations of the variables; basis weight, drying air temperature, and pressure drop. Numerous replicates were run for each combination of variables in order to ensure the repeatability of the test method. The results of the 242 experiments show drying times ranging from approximately 0.6 to 3.5 seconds at average drying rates ranging between approximately 110 and 300 kg/m^2h.

The experiments were carried out at the research facility of Metso Paper, Biddeford, Maine, USA, where a unique piece of equipment, well suited for the kind of experimental study described in this report, is located.

CONTENTS

1 Introduction

Through drying of tissue is a very costly operation, mainly owing to the high energy demand resulting from a high initial moisture ratio (approximately 3 kg/kg) of the web. The high initial moisture ratio is a result of the dewatering step. In through drying, dewatering is performed by passing the web across a series of vacuum slots and so called molding boxes, where the web is dewatered and drawn into the supporting fabric. In conventional Yankee drying the web is dewatered by pressing, and is then transferred to one or two large steam heated cast iron cylinders, which the web passes without any supporting fabric. The moisture ratio that is reached in the vacuum dewatering step of a through drying system is limited by the cost for applying the vacuum, which increases dramatically as the desired moisture ratio is lowered. However the vacuum dewatering and molding of the paper web into the fabric is also the essential advantage of through drying when compared to Yankee drying. In the molding process, the sheet is not compressed to the same extent as in the pressing operation and thus the result of through drying is a product showing much higher bulk and absorbency than a conventionally dried product. The intimate contact between the web and fabric in through drying also reduces in plane shrinkage.

In order to investigate the possibility to improve the energy demand of the process, modeling and understanding of the fundamental characteristics of the drying process is essential. These models need to be validated against experimental data. The aim of the present study was to provide such experimental data for through drying of paper tissue, at intensities comparing to industrial conditions. The experiments where performed at the research facility of Metso Paper in Biddeford, Maine, USA.

2 Experimental method

2.1 Equipment

A schematic drawing showing the equipment that was used in the present study is shown in Figure 1. The drying air is supplied from an electrically heated cylinder, approximately 0.4 m in inner diameter. In order to keep the pressure drop constant across the sheet during a test, the air in the cylinder is kept at pressure by a piston loaded with weights. To facilitate changes to the pressure drop across the sheet, the piston is counter weighted by a stack of easily accessible and exchangeable weights. A fan circulates air from the cylinder through an electric air heater, which prevents the development of temperature gradients in the cylinder and decreases the heat-up time between consecutive tests. As the piston is released, a bypass valve opens and for a short period of time, prior to the opening of the gate valve and the simultaneous closing of the bypass valve, air is bypassed to the surroundings. This procedure allows the piston to accelerate and pressure oscillations to decline before the gate valve is opened and the 5.08 cm (2 inch) diameter sample is exposed to the air flow. The moisture ratio of the supply air is measured using a humidity transmitter positioned at the compressed air supply inlet.

Data is collected using a high speed computer and data acquisition system, sampling data at a frequency of 240 Hz. The flow rate through the sheet is measured using a venturi tube placed below the sample. The pressure drops over the venturi tube and across the sample are monitored by using differential pressure transmitters. The exhaust static pressure is also monitored by a differential pressure transmitter. To monitor the vapor content of the exhaust air during an experiment, a spectrophotometer is positioned in the contraction of the venturi tube, where the temperature is also measured. The supply air temperature is measured in three positions above the sheet and the exhaust air temperature is measured in five positions, approximately 5 cm below the sheet. In addition, the air temperature in the cylinder is monitored in two positions. The temperature of the cylinder wall and that of the wall of the exhaust pipe are also monitored for control purposes.

The setup includes four separate temperature controllers and heating circuits, i.e. the cylinder wall temperature (heating blankets around the cylinder walls and cartridge heaters in the bottom plate), nozzle temperature (heating wire), cylinder air temperature (air heater in the circulation circuit), and the exhaust pipe temperature (heating wire) are all individually monitored and controlled. The heating of the exhaust pipe is necessary to prevent condensation of water vapor on the walls of the venturi tube and on the optics of the spectrophotometer.

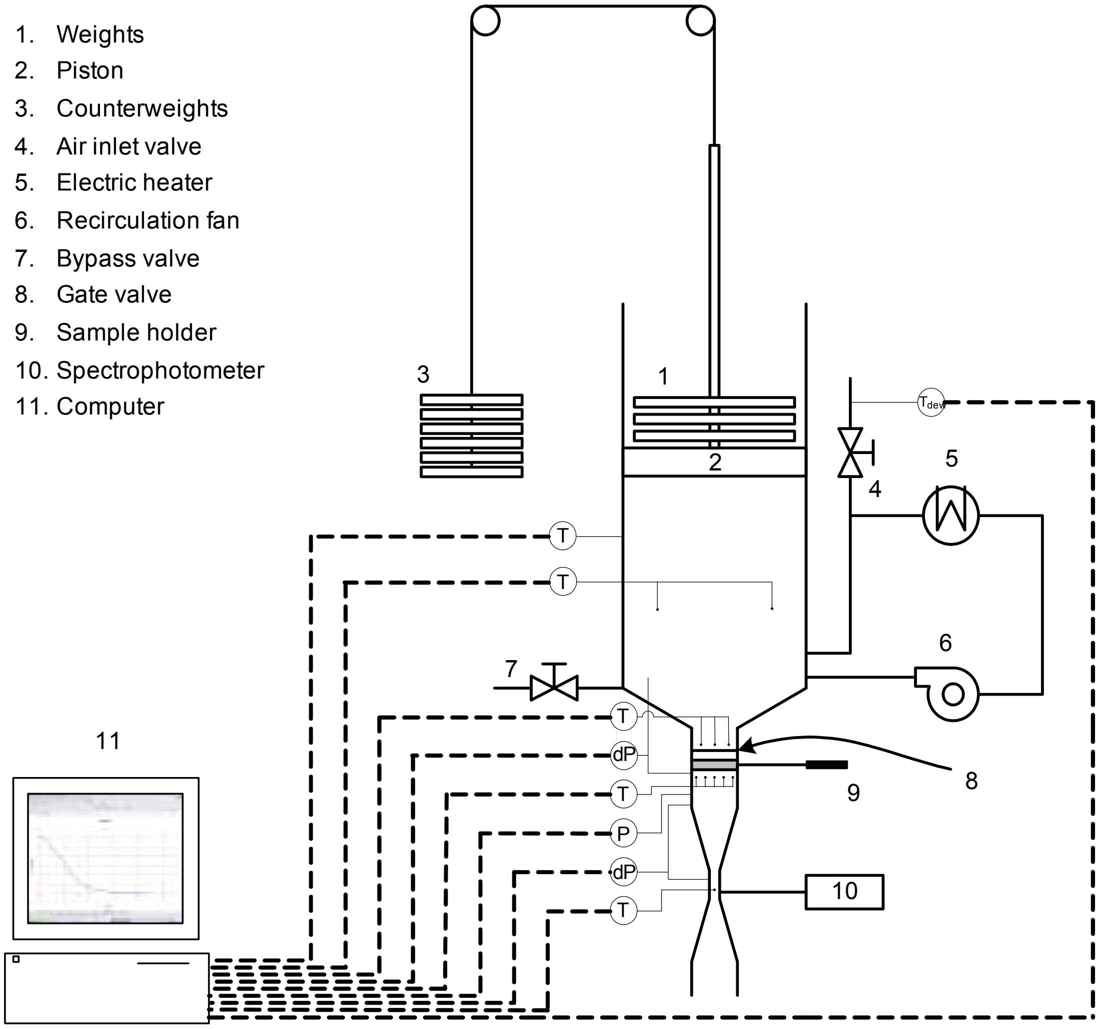

Figure 1. *Schematic representation of the through drying equipment and data acquisition system*

2.2 Sheet preparation

All samples in the current study where prepared using unrefined softwood kraft pulp. A sample of air dry pulp was dried at 120 ºC in order to determine the moisture content, which was normally in the range of 3 to 4% by weight, i.e. the sample was considered bone dry when dried at 120 ºC. Air dry pulp was then disintegrated in 2 liters of water at 3000 rpm to a total of 15000 revolutions. The pulp suspension was then diluted to a concentration at which, 0.5 liters of suspension corresponded to the mass of fiber needed for the simultaneous formation of three 5.08 cm (2”) diameter sheets, i.e for the three basis weights 20, 30 and 40 g/m^2 the concentrations were 0.24, 0.36 and 0.49 g/l respectively. The sheets where formed in a standard hand sheet mold, where the screen had been modified to produce three small sheets instead of one large, i.e. the screen was masked so that only three circles (5.08 cm in diameter) where open to flow.

According to Tietz (1992), vacuum dewatered sheets show a significantly different drying behavior than that of wet pressed sheets, i.e. a much more rapid increase in drying rate was found for the vacuum dewatered samples. In order to imitate the vacuum dewatering on an industrial machine, a small chamber was evacuated to o vacuum in the range of 50 to 80 kPa, depending on basis weight, and the sample was then subjected to a short through-flow of air resulting from letting the chamber equilibrate to atmospheric pressure. The pulse length was simply determined by the volume of the vacuum chamber, and was therefore not a controlled parameter.

The sheet was then carefully transferred to a balance, using a pair of tweezers. If the desired initial moisture ratio was not reached in the vacuum dewatering step, the sample was allowed to rest for a short time until the target weight was reached. The sample was then transferred to the sample holder (Figure 2) where it was supported by a piece of commercial TAD-fabric (Albany 46×29 GST-003, also branded as ProLux 003). It was observed that the fabric shrunk substantially when heated to temperatures above approximately 190 ºC, which where reached at the end of the high temperature tests in this study. Therefore, the fabric was preheated to 200 ºC before it was cut to fit the sample holder. This procedure ensured that the permeability of the fabric was the same during all tests, even during the tests at lower temperatures, where fabric shrinkage was not as prominent. In order to facilitate a proper line up of the sample in the sample holder, the fabric was painted black to increase the contrast between sheet and fabric. When the sample was lined up a Teflon ring with small radial teeth was attached to keep the sheet in place during drying (Figures 2 and 3).

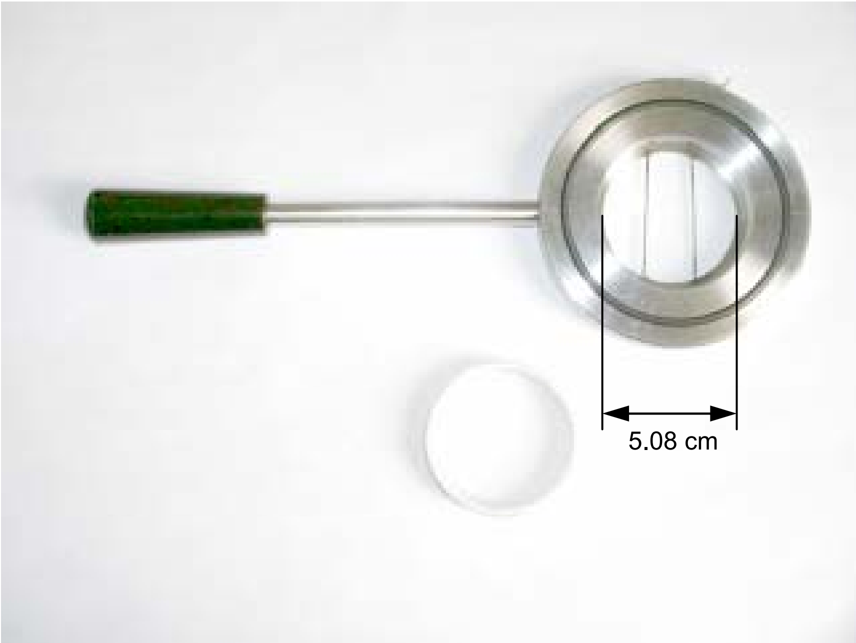

Figure 2. *The sample holder and the Teflon ring that holds the sheet in place during a test.*

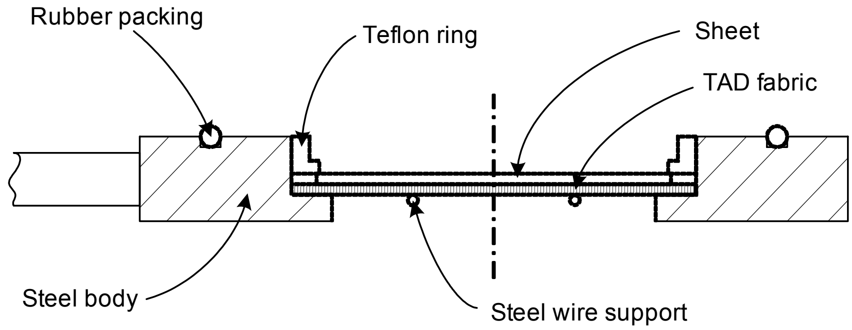

Figure 3. *Schematic drawing of the sample holder seen from the side (cut through center).*

2.3 Running a test

With the sheet properly lined up, the sample holder is put in place in the drying apparatus. As the test cycle starts, the sample holder is clamped in place by a pneumatic mechanism. Then the previously discussed by-pass valve opens and the piston starts moving. After a preset by-pass time, the by-pass valve is closed and simultaneously the gate valve is opened and air starts flowing through the sample. When the test time is reached the sample holder is automatically unclamped, the sample taken out and immediately weighed. The sample weights, recorded before and after the test, are used together with the information from the spectrophotometer to determine drying rate and moisture content as functions of time.

An example of typical plots of pressure drop and superficial velocity as functions of time is found in Figure 4. The corresponding moisture ratio of the exhaust air is shown in Figure 5.

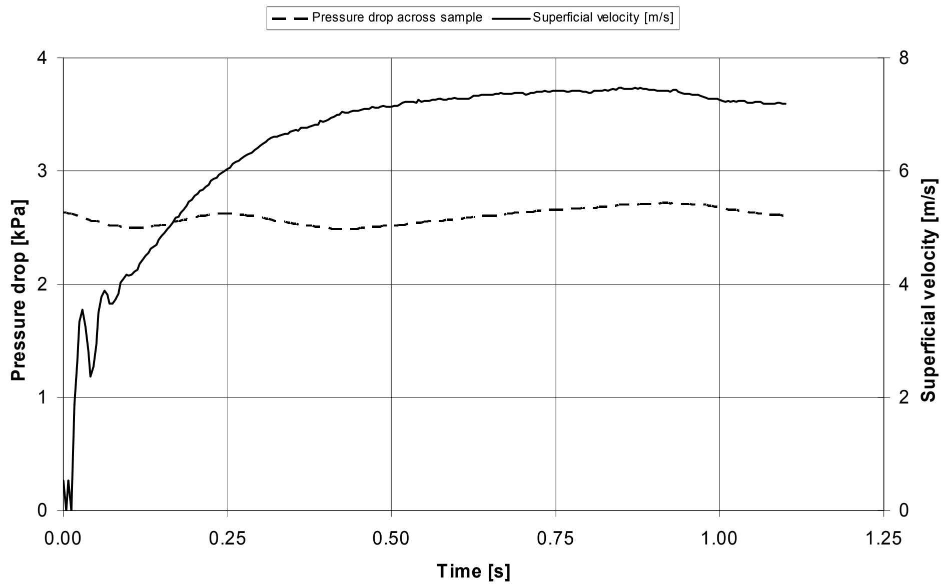

Figure 4. *Example of pressure drop and superficial velocity*

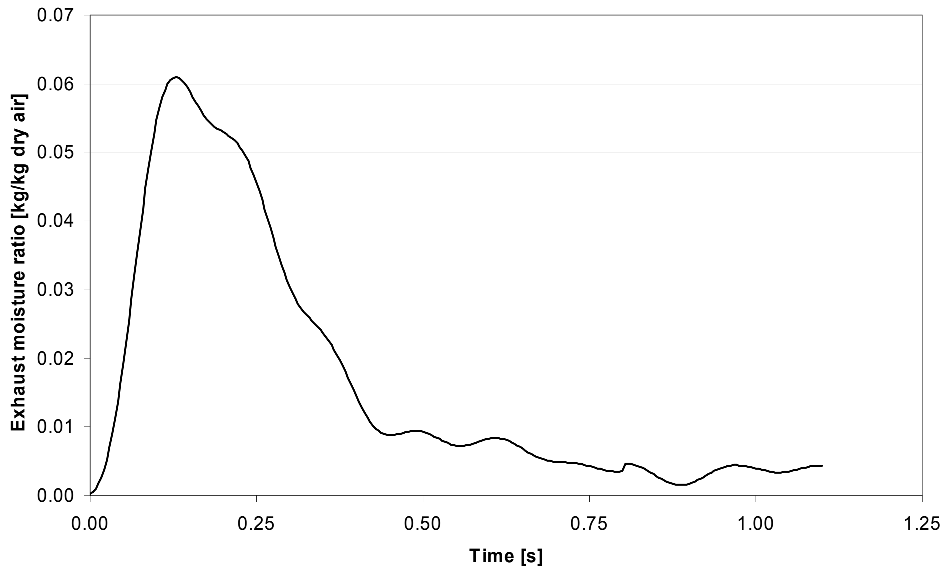

Figure 5. *Example of the air moisture content time profile*

Multiple tests where done to estimate the water lost in the procedure of transferring the sheet to the sample holder and finally to the dryer. The sample weights prior to drying where then corrected with this average water loss.

2.4 Varied parameters

Because the initial moisture ratio on industrial machines is about 3 kg/kg, the initial moisture ratio was kept approximately constant at that level (within the accuracy of sheet preparation). The basis weight was varied in three steps, i.e. 20, 30 and 40 g/m^2, which cover the range of most industrial applications. Three different supply air temperatures, i.e.

100, 150 and 200 ºC, were studied and two different levels of pressure drop were used for each combination of the other variables (basis weight and temperature), resulting in a total of 18 combinations of the three studied variables. Because of practical reasons, the two pressure drop levels where not the same for all three basis weights. For the two lower basis weights, pressure drops of 1.0 and 2.7 kPa across the sheet were used as the two pressure drop levels. For the highest basis weight however, a pressure drop of 1.0 kPa resulted in such low drying rates that the air volume in the cylinder was not enough to completely dry the sample. Thus, for the 40 g/m^2 samples the low and high pressure drop levels where 2.7 and 5.0 kPa respectively. As a result, there was one common pressure drop, i.e. 2.7 kPa, for all three basis weights. In order to ensure repeatability, a number of replicates were run for each combination. Due to problems, e.g. sample line up, incorrect initial moisture ratio and problems with the data acquisition, not every run resulted in a successful experiment, i.e. well over 400 runs were done of which 242 are presented in this report. The problems described above, is the reason why the number of experiments for each combination of variables varied between 10 and 18 in this study. The supply air moisture ratio was simply that of the compressed air supply, i.e. approximately 0.003 kg/kg dry air for all runs. The different combinations of the studied variables are shown in Table 2.

Table 2. *Studied variables*

Basis weight [g/m²]	Pressure drop [kPa]	Temperature [ºC]
20	1.0	100
		150
		200
	2.7	100
		150
		200
30	1.0	100
		150
		200
	2.7	100
		150
		200
40	2.7	100
		150
		200
	5.0	100
		150
		200

3 Data evaluation

The sampled data were evaluated by using a computer program written in Excel's Visual Basic environment. The program reads the temperature data, pressure data and the raw spectrophotometer data and then calculates the flow rate, the drying rate and moisture ratio of the sheet as a function of time, based on the weight of the sheet before and after drying.

The spectrometer is used only to get the shape of the drying rate curve, whereas the total amount of evaporated water originates from the sample weight before and after drying. Due, to the noise level of the spectrophotometer data, the signal needs to be filtered during the data evaluation. For this purpose, the discrete Fourier transform of the data was calculated using a Fast Fourier Transform algorithm (FFT) and higher frequencies were then cut off. The result of this kind of filtering depends on the cut off frequency. If the cut off frequency is relatively high, the result is a relatively low filtering level, i.e. data still shows a lot of noise. If on the other hand, the cut off frequency is relatively low the resulting drying rate curve is smoother, but may have lost a lot of the original characteristics of the unfiltered data. Thus, it is important to choose a filter level which gives a good smoothing of data without changing its general characteristics. In this study this choice was done manually by inspection. For future work it is desirable to apply a suitable numeric algorithm that makes this choice. Examples of two filter levels compared to the unfiltered data are shown in Figure 6. It is clear how the filter level affects the general characteristics of the resulting drying rate curve.

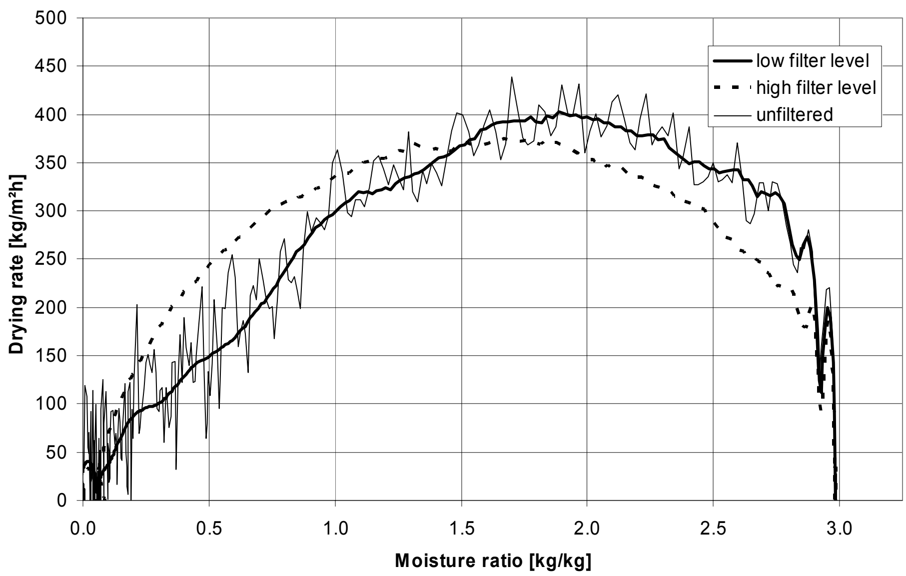

Figure 6. *Effect of filter level on the drying rate curve.*

4 Repeatability

4.1 Hand sheet preparation

The actual basis weights of the hand sheets, prepared according to the method described previously, agree well with the desired basis weights, which is reflected by the average basis weights and 95% confidence intervals presented in table 3.

In this study the aim was to keep the initial moisture ratio at 3 kg/kg for all samples but, because of the relatively primitive dewatering equipment, there was a relatively large variation in actual initial moisture ratios.

Table 3. *Average basis weight and standard deviation*

Desired basis weight (g/m^2)	Average basis weight (g/m^2)	Standard deviation (g/m^2)
20	19.9	0.78
30	30.5	0.90
40	40.3	1.3

Table 4. *Average initial moisture ratio and standard deviation*

Desired basis weight (g/m^2)	Average initial moisture ratio (kg/kg)	Standard deviation (kg/kg)
20	3.03	0.14
30	2.91	0.13
40	2.92	0.12

4.2 Drying method

All experimental results presented in this study are based on individually prepared hand sheets. By nature, paper is a non-uniform material and each sheet has its own unique structure and therefore it is not likely that any two samples of the same basis weight and with the same initial moisture ratio will yield exactly the same drying result. As a consequence, it is difficult to assess the repeatability of the entire experimental method from pulp to dry sheet. The only means by which the repeatability of the method may be evaluated is by inspection of the results, a process which of course is rather subjective. In this study however, approximately ten to twelve replicates where run for each studied set of test variables and in all cases, i.e. for all sets of variables, the spread in data was found acceptable. However, it should be noted that the variation in data was observed to increase with increasing drying intensity, which in turn is a result of approaching the limits of the equipment.

5 Results

In order to show the effect of various parameters, the average drying rate curves for each combination of the studied variables is shown in the section. The average is used simply since it is not practical to show and compare the data from numerous experiments in the same figure. However, the original data corresponding to the individual samples are found in Appendixes 1, 2 and 3.

Finding an average drying rate curve that represents the average drying behavior of a set of data is not as easy as it might seem at first. Because of variations in the sheet preparation step, initial moisture ratio and basis weight were not exactly the same for different runs, even though they were ideally supposed to be. As shown in Table 3 above, the variation in basis weight was rather small. It was assumed here that the magnitude of the variation of initial moisture ratio in this study (at the most about 0.5 kg/kg) does not affect the principle shape of the drying rate curve. The results are ordered such that, for each combination of basis weight and pressure drop, drying rate curves for the three studied inlet air temperatures are displayed in the same figure.

The drying rate curves show an initial rapid increase followed by a period of slower increase before the maximum drying rate is reached and the falling rate begins at a moisture ratio of approximately 1.5 kg/kg (Figures 7 to 12). When the temperature is raised from 100 to 200 ºC the peak drying rate increases by approximately 180%. Generally, the results follow the expected trend; that more intense conditions yield higher drying rates. However, the results for the 20 g/m^2 at 200 ºC sheets at a pressure drop of 1.0 kPa (Figure 11) show much lower drying rates compared to the lower temperature levels than what is generally found for the other experimental series in this study (Figures 7, 8, 9, 10 and 12). There is no apparent reason why there should be a trend difference for this particular experimental series, and the reason for the problem is so far unidentified.

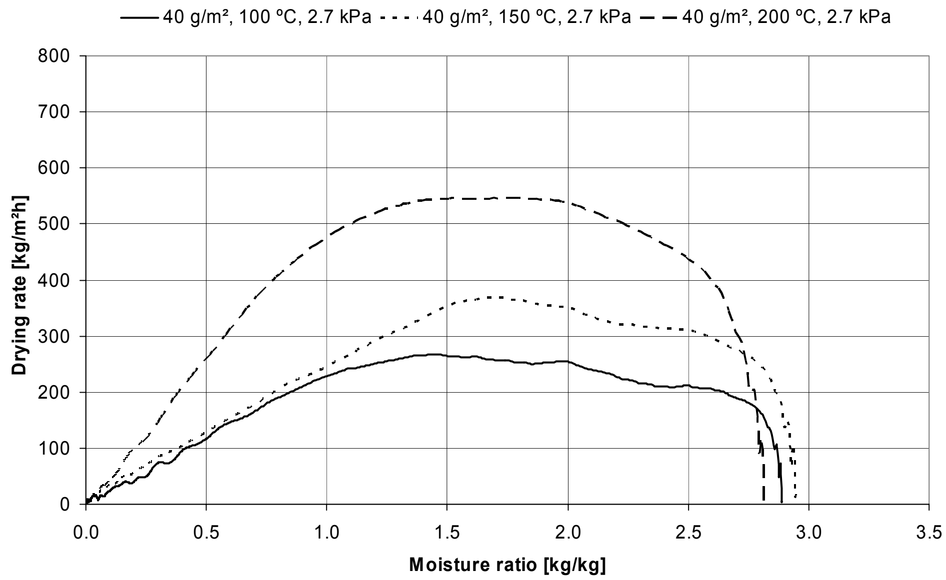

Figure 7. *Drying rate vs. moisture ratio for 40g/m^2 sheets at 2.7 kPa pressure drop*

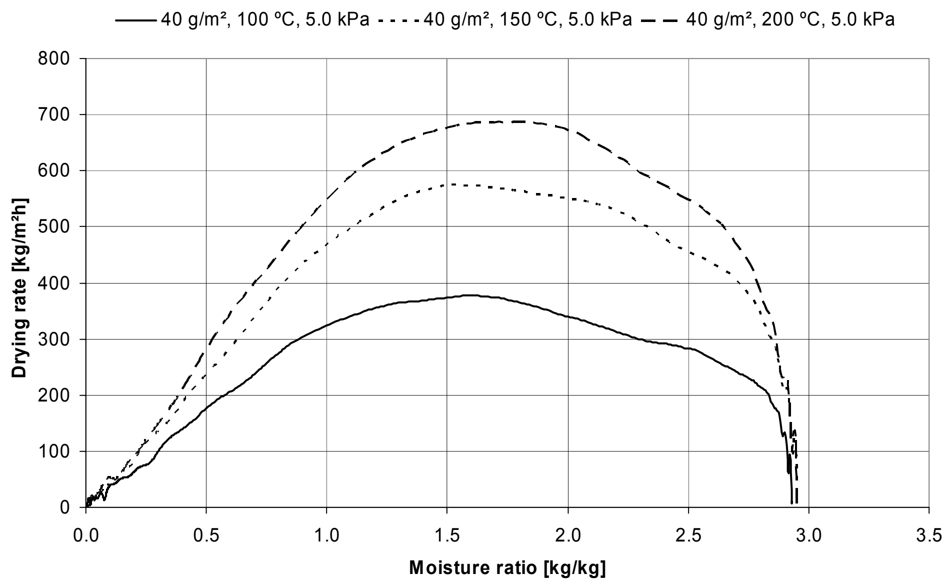

Figure 8. *Drying rate vs. moisture ratio for 40g/m^2 sheets at 5.0 kPa pressure drop*

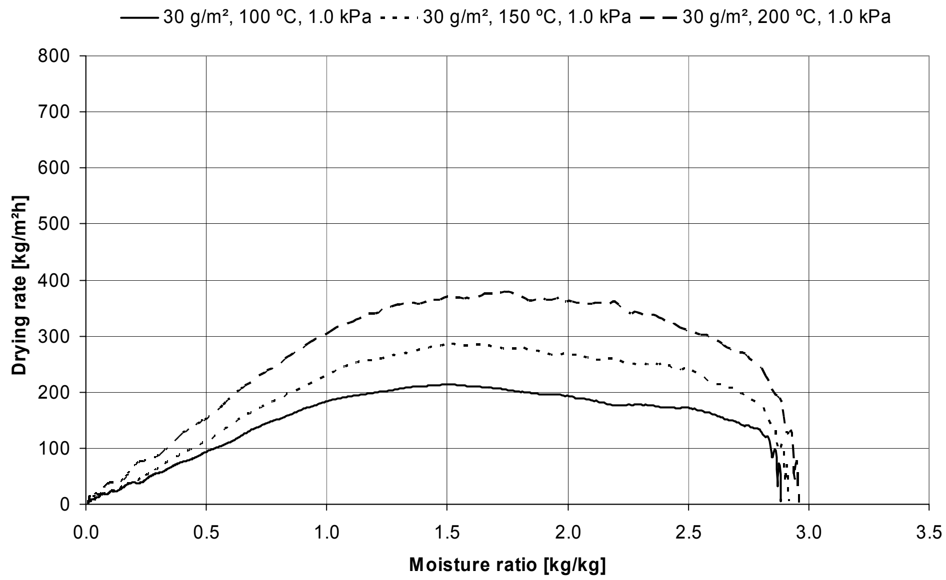

Figure 9. *Drying rate vs. moisture ratio for 30g/m² sheets at 1.0 kPa pressure drop*

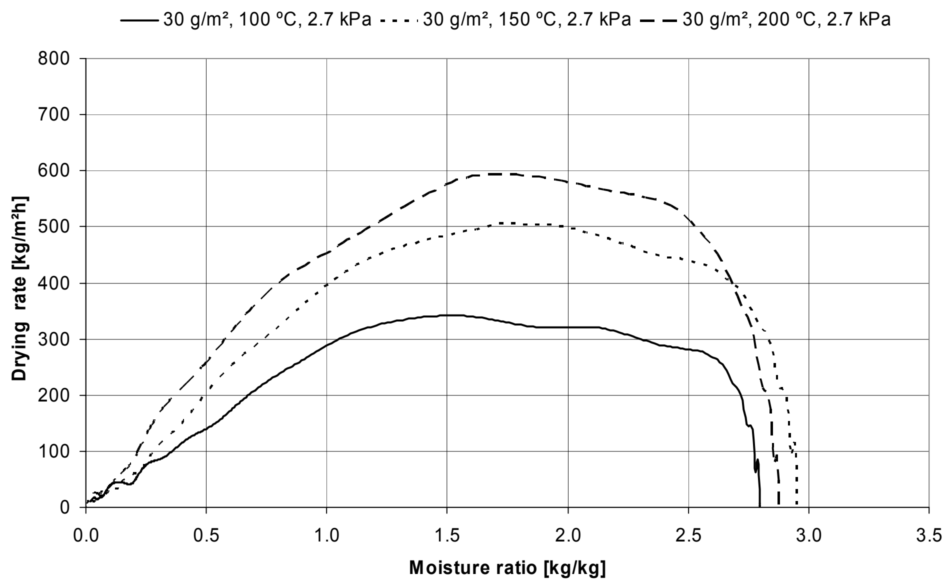

Figure 10. *Drying rate vs. moisture ratio for 30g/m² sheets at 2.7 kPa pressure drop*

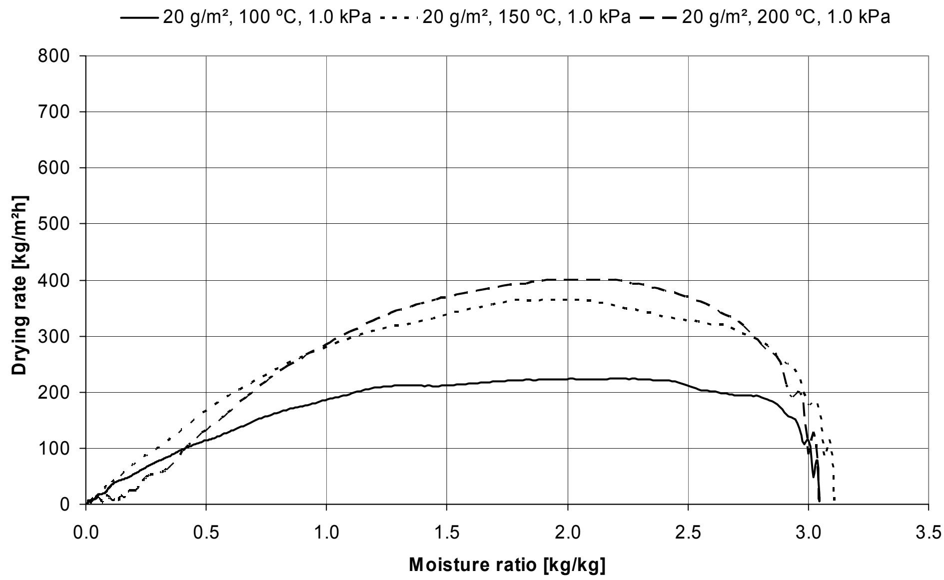

Figure 11. *Drying rate vs. moisture ratio for 20g/m² sheets at 1.0 kPa pressure drop*

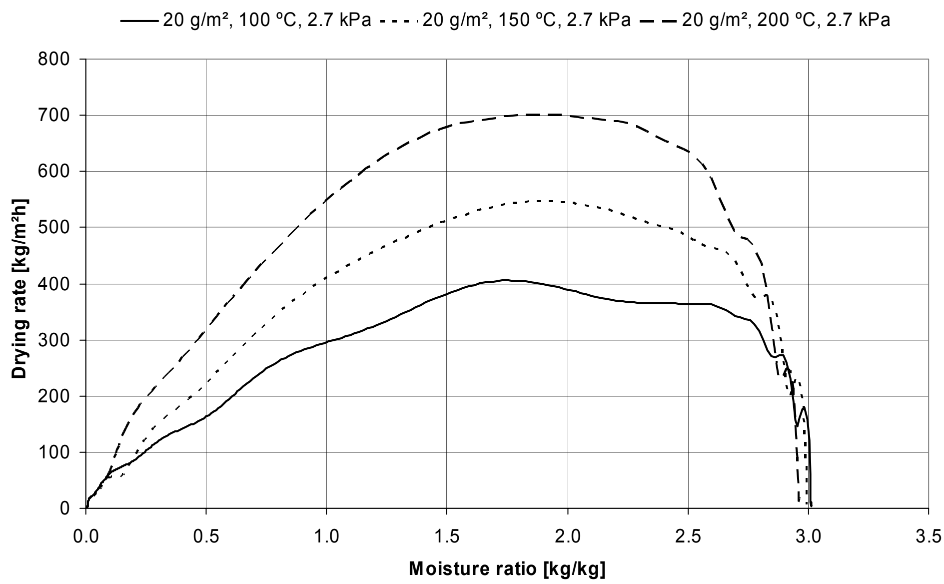

Figure 12. *Drying rate vs. moisture ratio for 20g/m² sheets at 2.7 kPa pressure drop*

As mentioned previously, because of practical reasons, it was not possible to run all of the 20, 30 and 40 g/m² samples at the same two pressure drops. However, the pressure drop 2.7 kPa was a common pressure drop for all three studied basis weights. The average drying rates for these samples (average over the drying time) is shown for the different inlet temperatures in Figure 13. When calculating the average drying rates, the time to reach a moisture ratio of 0.01 kg/kg was used as the averaging time. Using a lower moisture ratio criterion will only introduce a greater error since uncertainty increases rapidly at the end of drying, when the drying rate is very low.

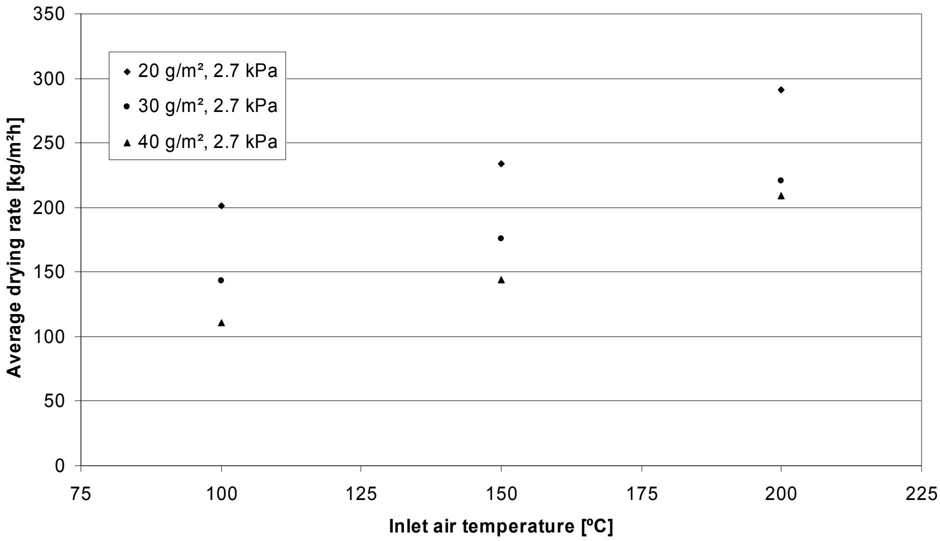

Figure 13. *Average drying rates for different basis weights at different inlet air temperatures*

The permeability of dry sheets was also studied using a Frazier Fabric Permeability Machine 360. Six samples from each of the three basis weights were studied by applying a pressure difference across the sheet and simultaneously measuring the flow rate. The results (averages of the six samples of each basis weight) are shown in Figure 14. For flow through porous media, the pressure drop is often written as

$$\frac{\Delta P}{L} = Cu^n, \tag{1}$$

where C is a regression constant and u is the superficial velocity and the exponent n is normally in the range between 1 and 2. If n equals 1 the equation reduces to the viscous part of the Forchheimer relation (Eq. 2.)

$$\frac{\Delta P}{L} = \alpha\mu u + \beta\rho u^2 \tag{2}$$

If on the other hand the value of n lies in the range between 1 and 2, the flow is no longer purely viscous and the inertial term in the Forcheimer relation can no longer be neglected. The values of the exponent n, calculated from the permeability experiments, are shown in Figure 14. The inertial contribution is rather high but decreases somewhat with basis weight, which is expected because of the lower flow rate. The values of the exponent n determined in this study are much higher than those found in previously published data (Polat 1989). For basis weights 25 and 50 g/m^2 Polat reported 1.24 and 1.07 as values of the exponent *n,* values considerably lower than those presented in Figure 14.

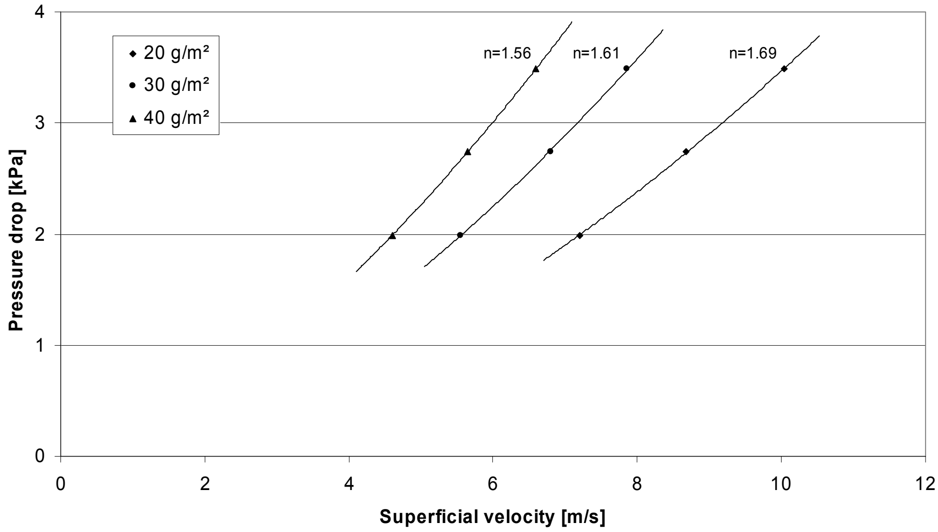

Figure 14. *Pressure drop vs. superficial velocity for the permeability tests (Average values)*

6 Conclusions and future work

Experimental results at intensities corresponding to industrial conditions, i.e. high drying air temperature and constant pressure drop, were reported. Under these conditions, the entire drying process as short as 0.5 seconds was successfully monitored and recorded. Maximum and average drying rates as high as 700 kg/m^2h and 300 kg/m^2h respectively where recorded. This is in the region of what is found in industrial applications where average drying rates are normally in the range of 90 (Cui and Ramaswamy,1999) to 550 kg/m^2h (Karlsson and Oyj, 2000).

The experimental results from this study will be used for validation of a computer model for through drying at constant pressure drops. The future aim is that the model can be used when studying the energy optimization of the entire through drying process.

7 References

Cui,Y., and Ramaswamy, S. 1999. Through-air drying of tissue and towel grades. *TAPPI Journal* 82(4):203-208

Karlsson, M. 2000 Papermaking Part 2, Drying, vol. 9, p19, Helsinki: Fapet Oy

Polat, O. 1989. Trough drying of paper. Ph.D dissertation, McGill Univ., Montreal

Tietz, M. 1992. Durchströmungstrocknung von Papier, Ph.D. dissertation, Univ. of Karlruhe, Germany

Appendix 1

(40 g/m^2, 100 ºC, 2.7 kPa)

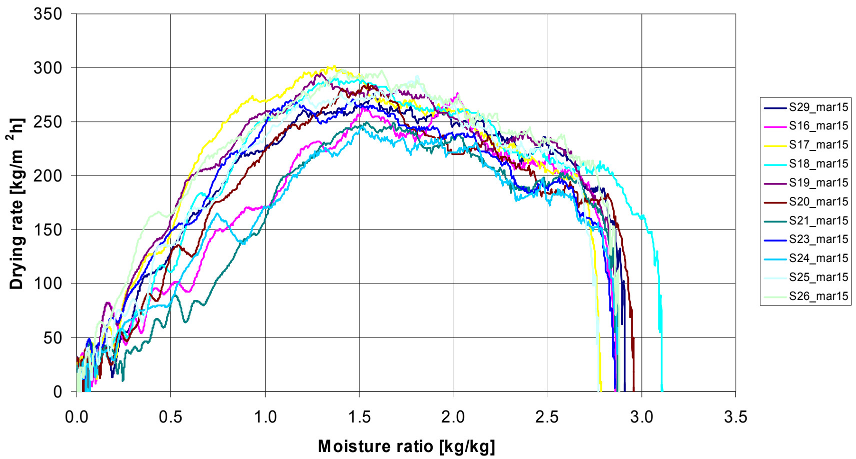

(40 g/m^2, 100 ºC, 2.7 kPa)

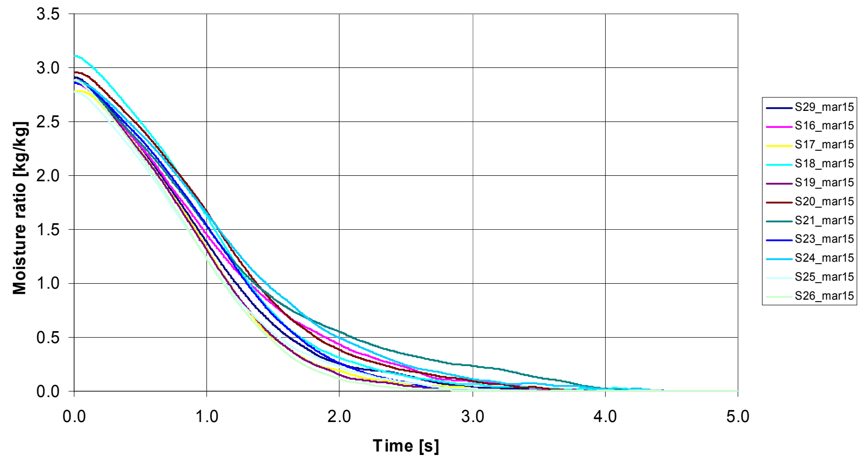

(40 g/m^2, 150 ºC, 2.7 kPa)

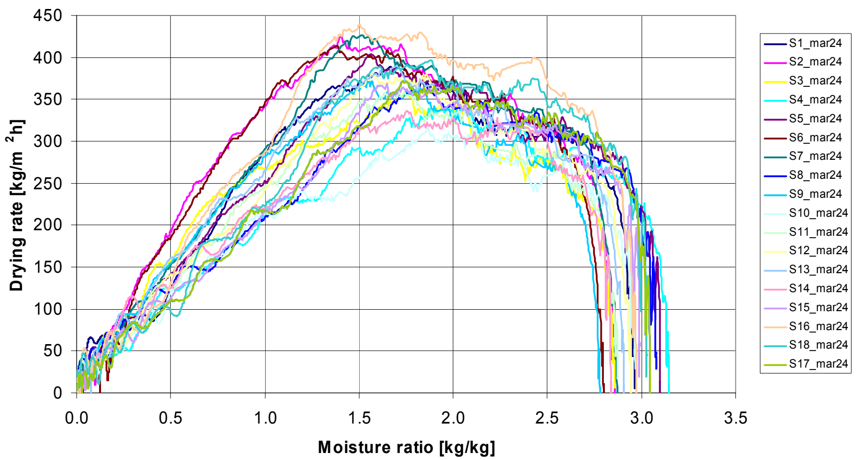

(40 g/m^2, 150 ºC, 2.7 kPa)

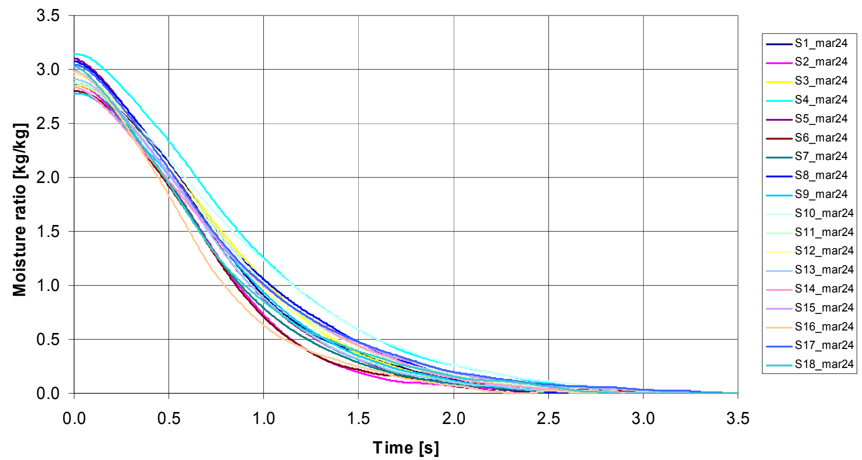

Appendix 1

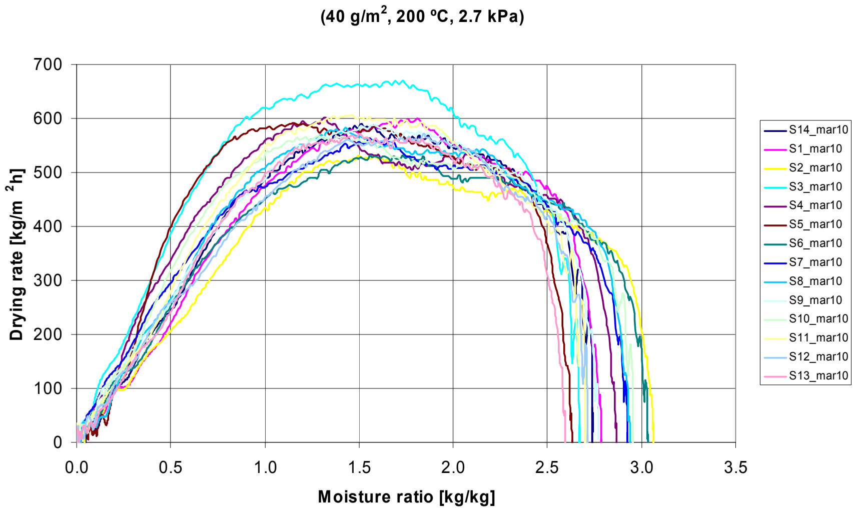
(40 g/m2, 200 ºC, 2.7 kPa)
Drying rate [kg/m 2h]
Moisture ratio [kg/kg]
S14_mar10
S1_mar10
S2_mar10
S3_mar10
S4_mar10
S5_mar10
S6_mar10
S7_mar10
S8_mar10
S9_mar10
S10_mar10
S11_mar10
S12_mar10
S13_mar10

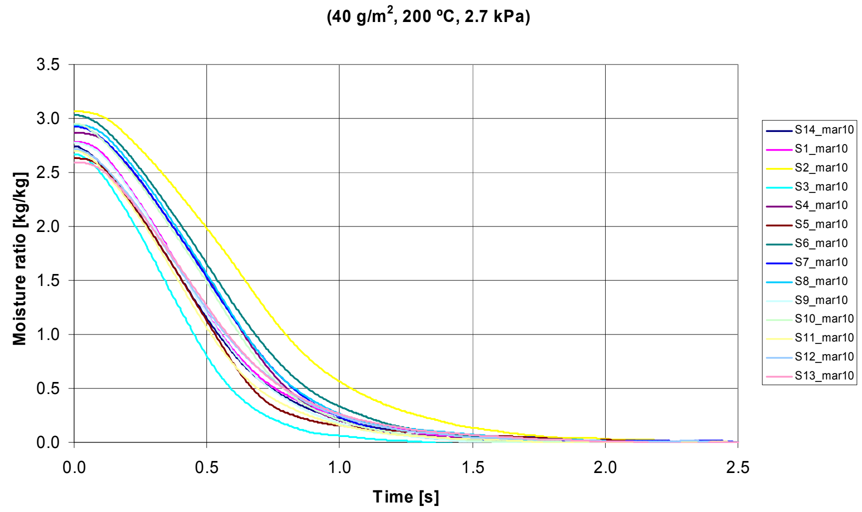
(40 g/m2, 200 ºC, 2.7 kPa)
Moisture ratio [kg/kg]
Time [s]
S14_mar10
S1_mar10
S2_mar10
S3_mar10
S4_mar10
S5_mar10
S6_mar10
S7_mar10
S8_mar10
S9_mar10
S10_mar10
S11_mar10
S12_mar10
S13_mar10

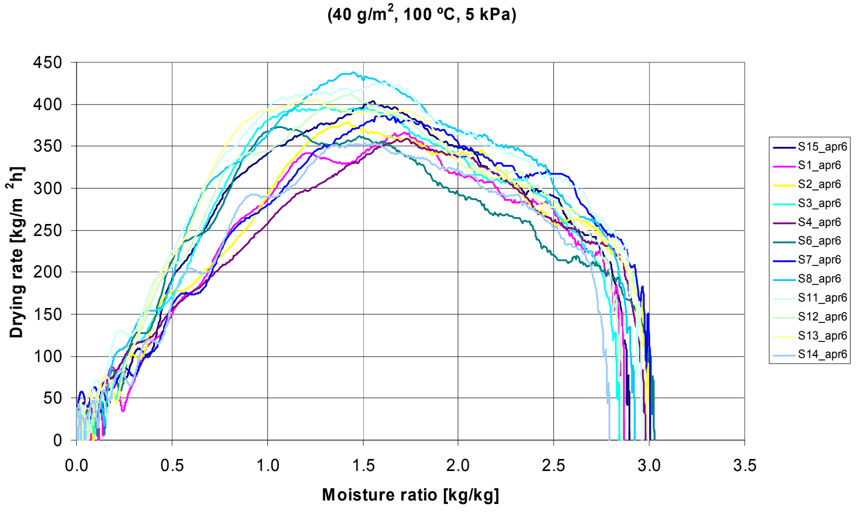
(40 g/m^2, 100 ºC, 5 kPa)
Drying rate [kg/m ^{2}h]
Moisture ratio [kg/kg]
S15_apr6
S1_apr6
S2_apr6
S3_apr6
S4_apr6
S6_apr6
S7_apr6
S8_apr6
S11_apr6
S12_apr6
S13_apr6
S14_apr6

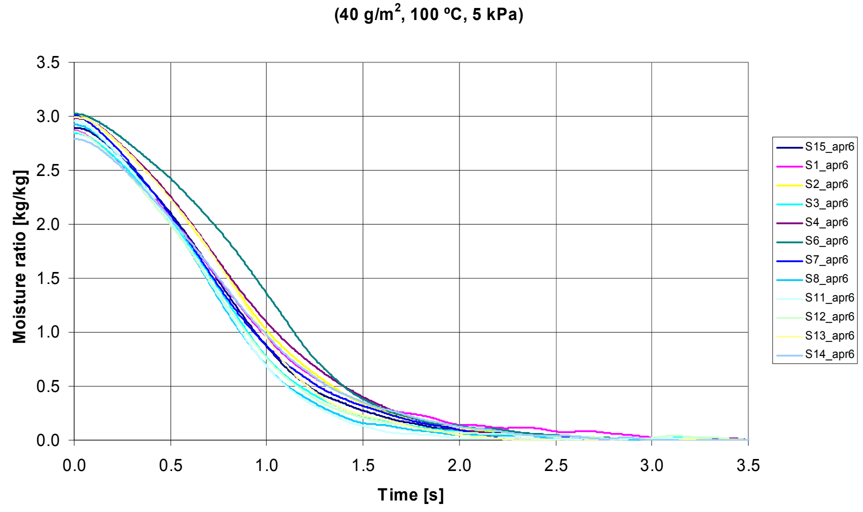
(40 g/m^2, 100 ºC, 5 kPa)
Moisture ratio [kg/kg]
Time [s]
S15_apr6
S1_apr6
S2_apr6
S3_apr6
S4_apr6
S6_apr6
S7_apr6
S8_apr6
S11_apr6
S12_apr6
S13_apr6
S14_apr6

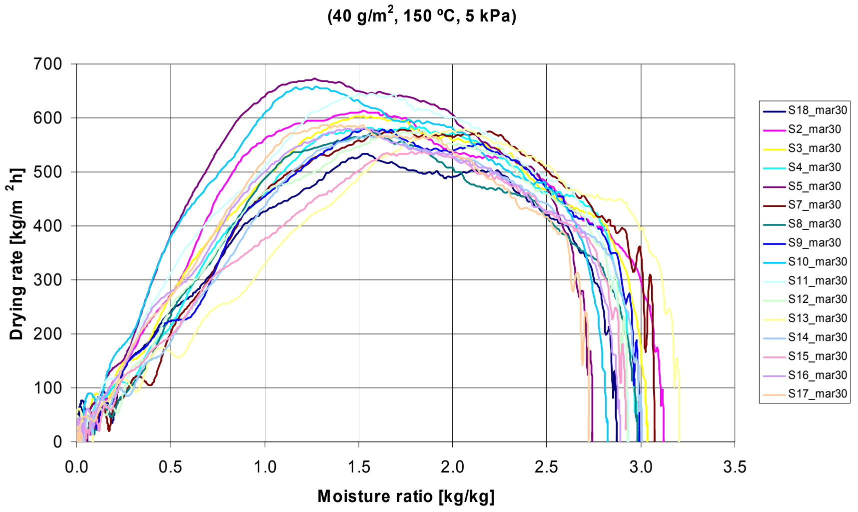
(40 g/m^2, 150 ºC, 5 kPa)
Drying rate [kg/m ^{2}h]
Moisture ratio [kg/kg]
S18_mar30
S2_mar30
S3_mar30
S4_mar30
S5_mar30
S7_mar30
S8_mar30
S9_mar30
S10_mar30
S11_mar30
S12_mar30
S13_mar30
S14_mar30
S15_mar30
S16_mar30
S17_mar30

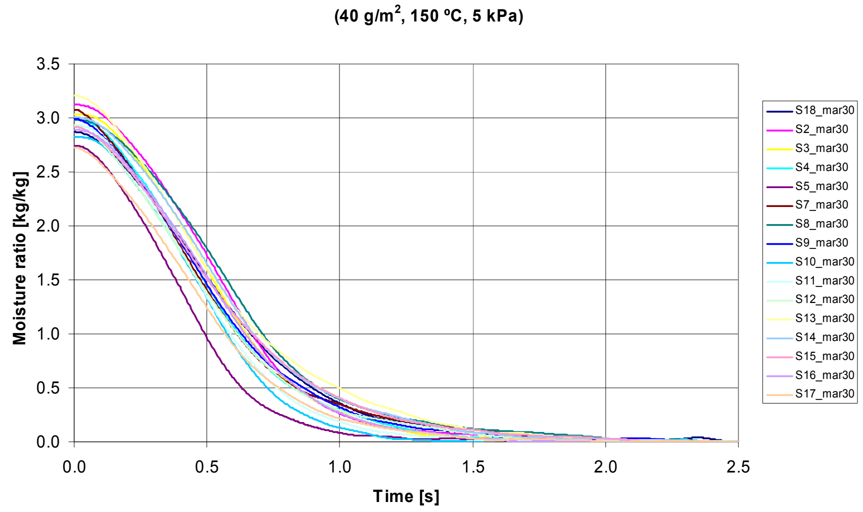
(40 g/m^2, 150 ºC, 5 kPa)
Moisture ratio [kg/kg]
Time [s]
S18_mar30
S2_mar30
S3_mar30
S4_mar30
S5_mar30
S7_mar30
S8_mar30
S9_mar30
S10_mar30
S11_mar30
S12_mar30
S13_mar30
S14_mar30
S15_mar30
S16_mar30
S17_mar30

Appendix 1

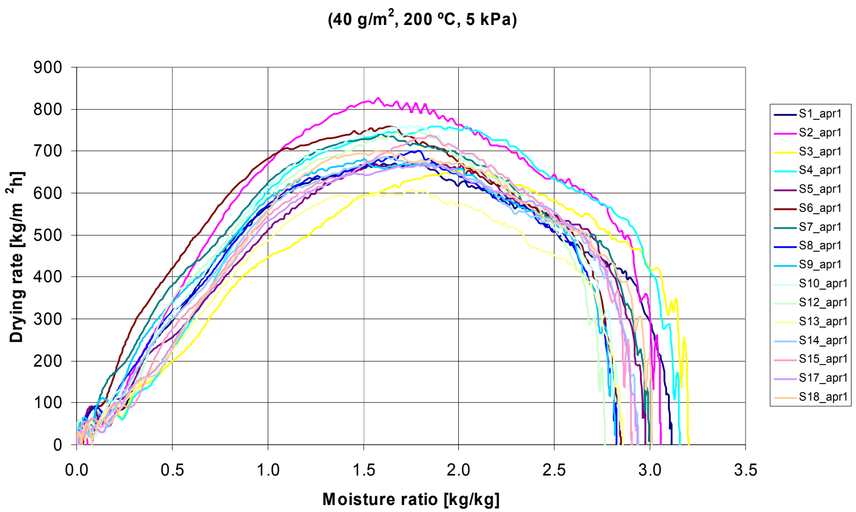
(40 g/m², 200 °C, 5 kPa)
Drying rate [kg/m ²h]
Moisture ratio [kg/kg]
S1_apr1
S2_apr1
S3_apr1
S4_apr1
S5_apr1
S6_apr1
S7_apr1
S8_apr1
S9_apr1
S10_apr1
S12_apr1
S13_apr1
S14_apr1
S15_apr1
S17_apr1
S18_apr1

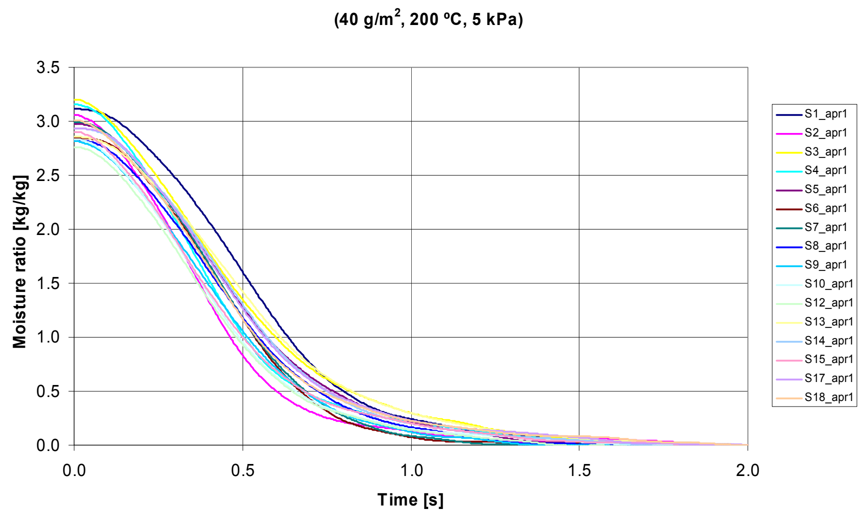
(40 g/m², 200 °C, 5 kPa)
Moisture ratio [kg/kg]
Time [s]
S1_apr1
S2_apr1
S3_apr1
S4_apr1
S5_apr1
S6_apr1
S7_apr1
S8_apr1
S9_apr1
S10_apr1
S12_apr1
S13_apr1
S14_apr1
S15_apr1
S17_apr1
S18_apr1

Appendix 1

Appendix 2

(30 g/m^2, 100 ºC, 1.0 kPa)

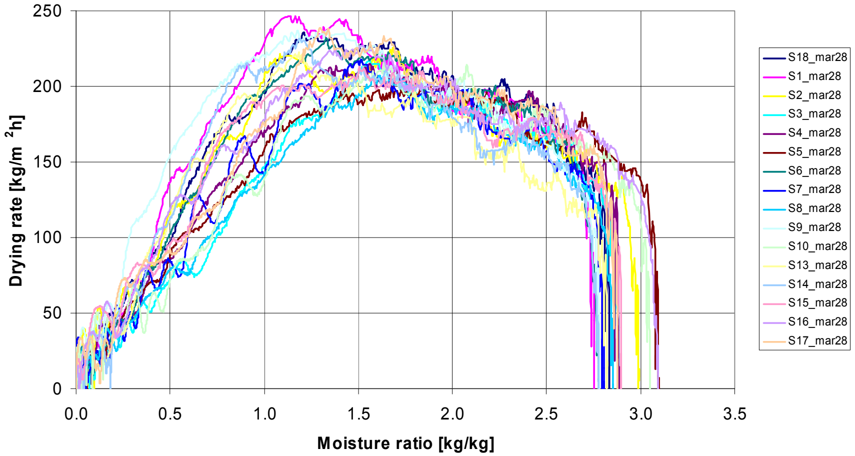

(30 g/m^2, 100 ºC, 1.0 kPa)

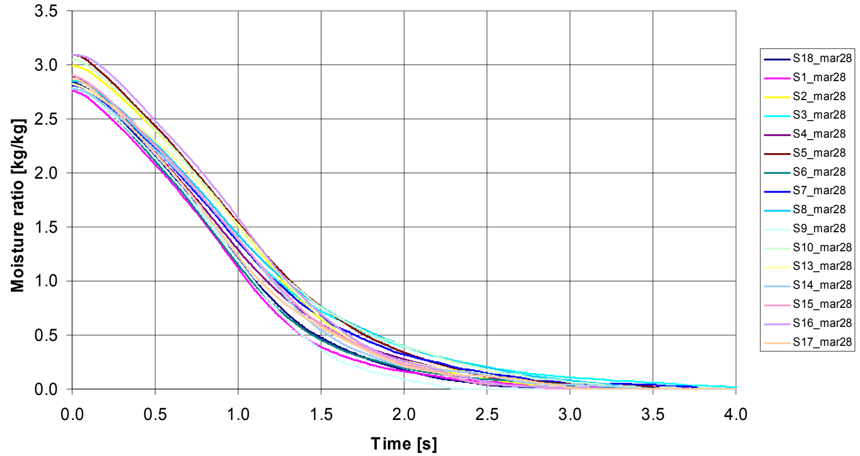

(30 g/m^2, 150 ºC, 1.0 kPa)

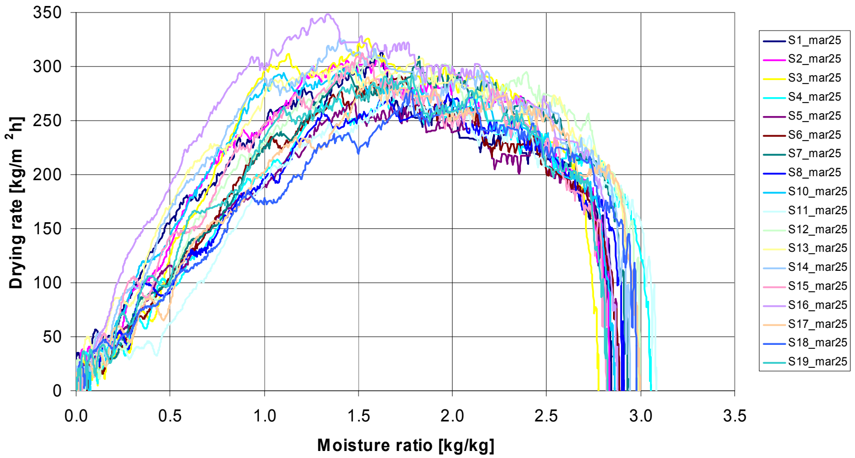

(30 g/m^2, 150 ºC, 1.0 kPa)

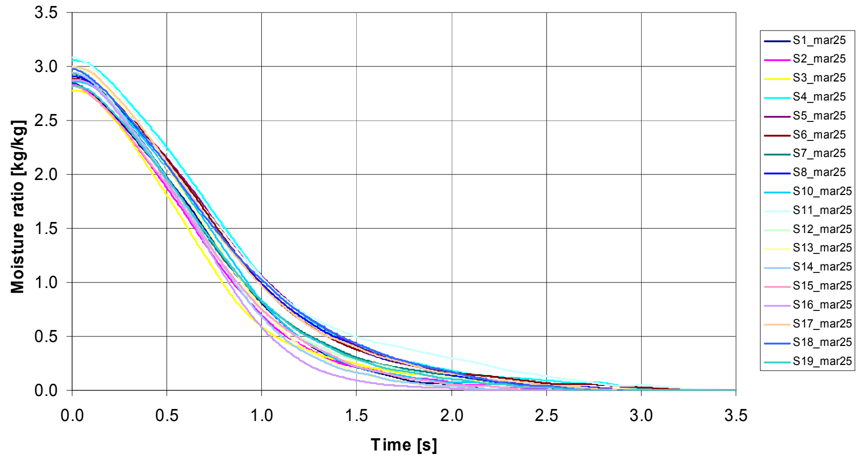

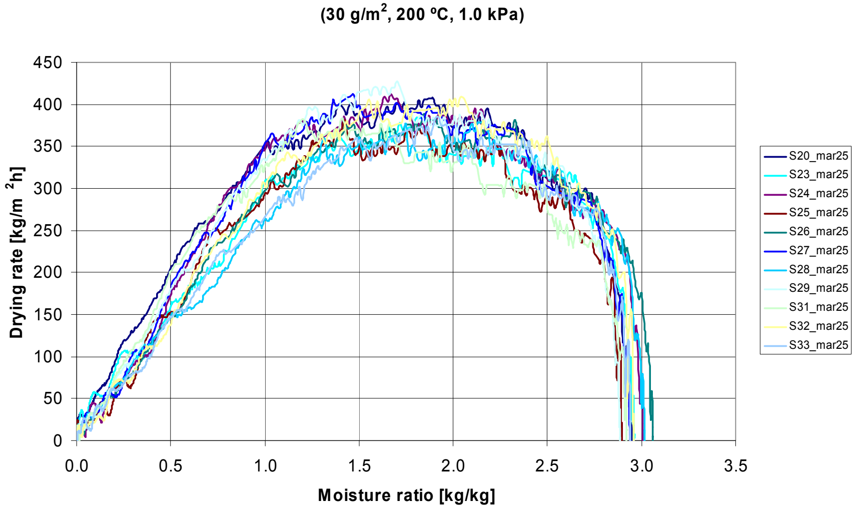
(30 g/m2, 200 ºC, 1.0 kPa)
Drying rate [kg/m2h]
Moisture ratio [kg/kg]
0
50
100
150
200
250
300
350
400
450
0.0
0.5
1.0
1.5
2.0
2.5
3.0
3.5
S20_mar25
S23_mar25
S24_mar25
S25_mar25
S26_mar25
S27_mar25
S28_mar25
S29_mar25
S31_mar25
S32_mar25
S33_mar25

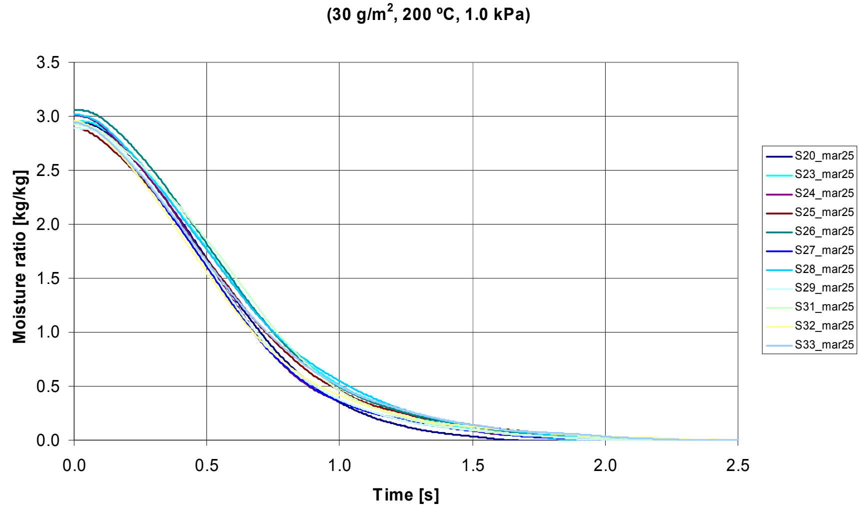
(30 g/m2, 200 ºC, 1.0 kPa)
Moisture ratio [kg/kg]
Time [s]
0.0
0.5
1.0
1.5
2.0
2.5
3.0
3.5
0.0
0.5
1.0
1.5
2.0
2.5
S20_mar25
S23_mar25
S24_mar25
S25_mar25
S26_mar25
S27_mar25
S28_mar25
S29_mar25
S31_mar25
S32_mar25
S33_mar25

Appendix 2

(30 g/m², 100 ºC, 2.7 kPa)

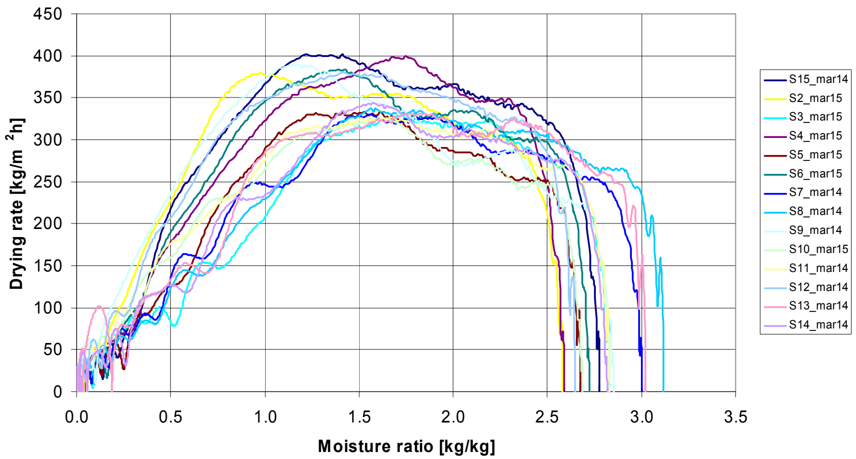

(30 g/m², 100 ºC, 2.7 kPa)

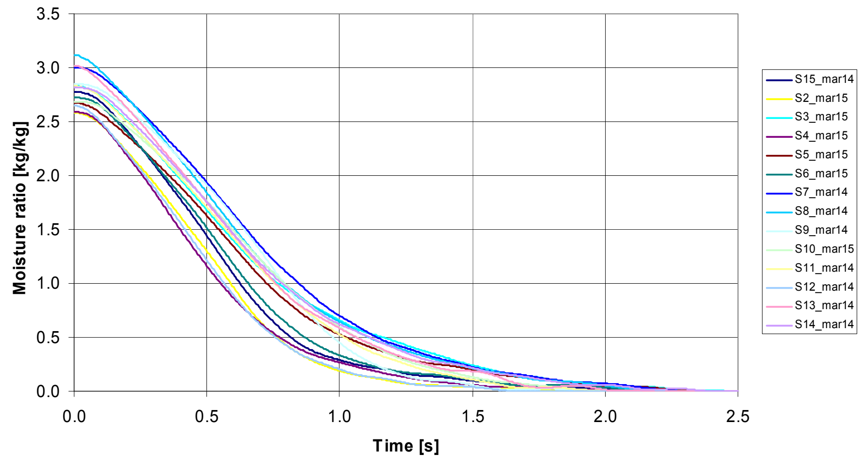

(30 g/m², 150 ºC, 2.7 kPa)

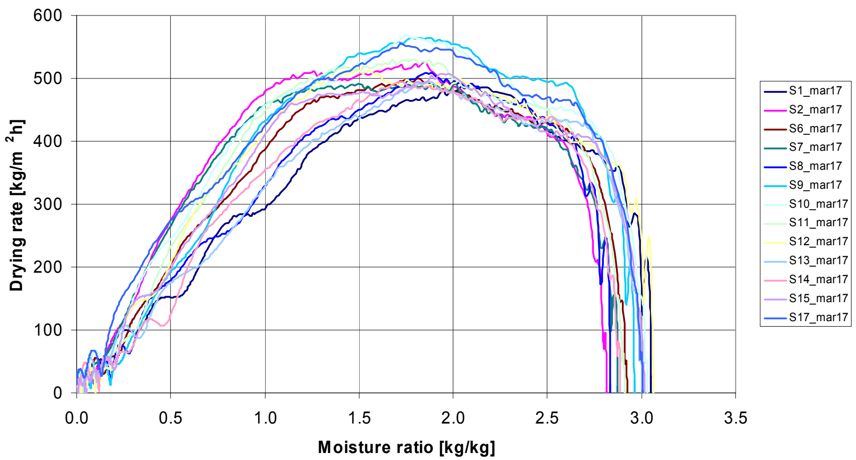

(30 g/m², 150 ºC, 2.7 kPa)

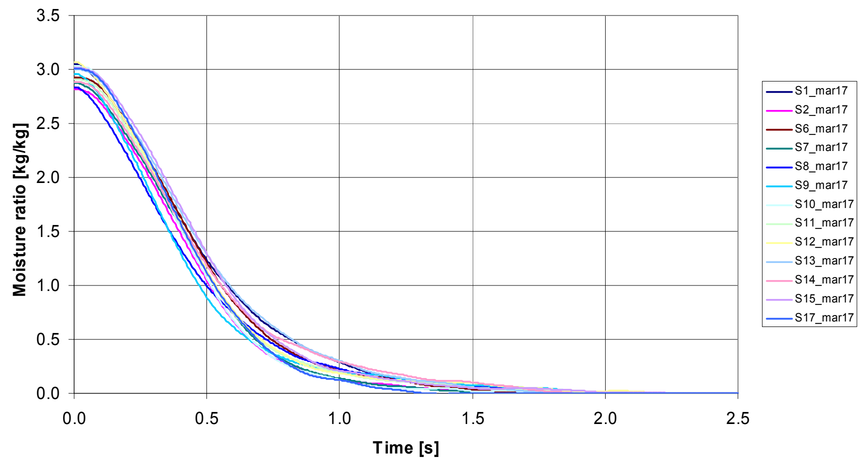

Appendix 2

Appendix 2

(30 g/m^2, 200 ºC, 2.7 kPa)

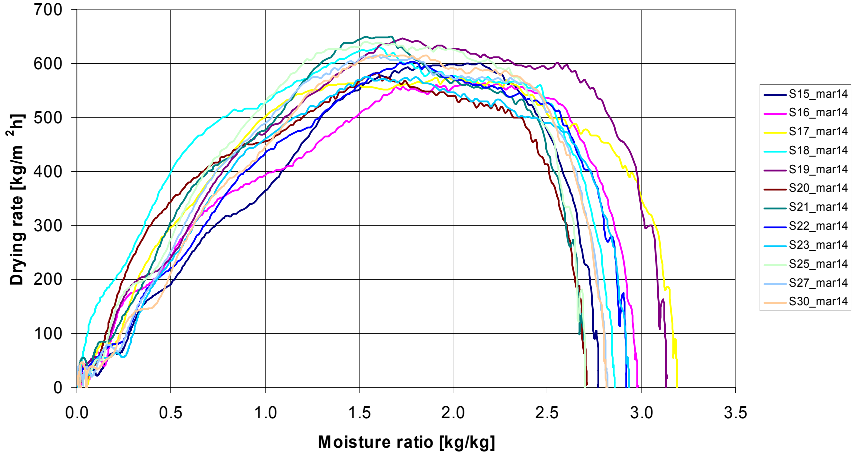

(30 g/m^2, 200 ºC, 2.7 kPa)

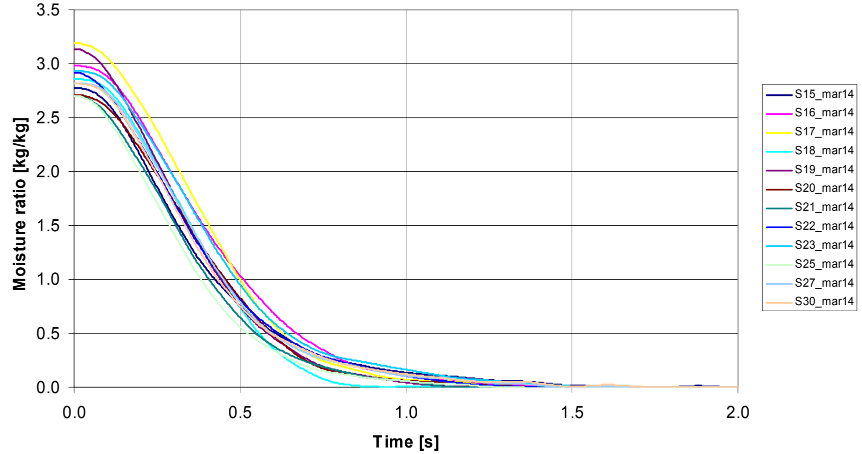

Appendix 3

(20 g/m^2, 100 ºC, 1.0 kPa)

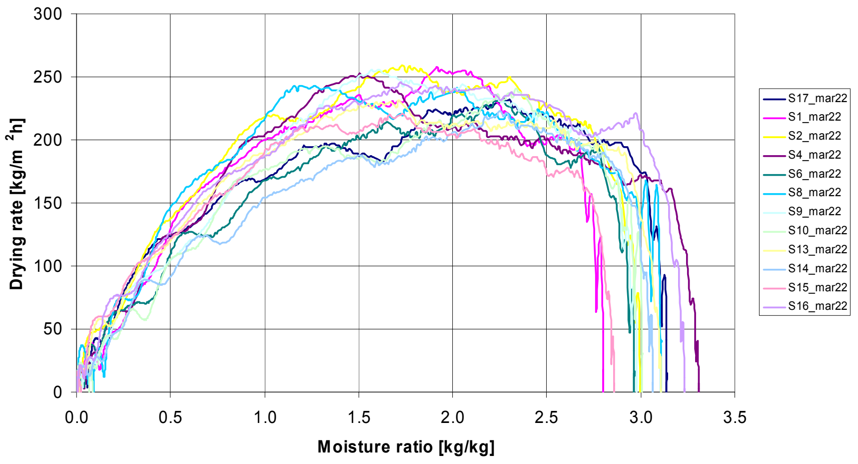

(20 g/m^2, 100 ºC, 1.0 kPa)

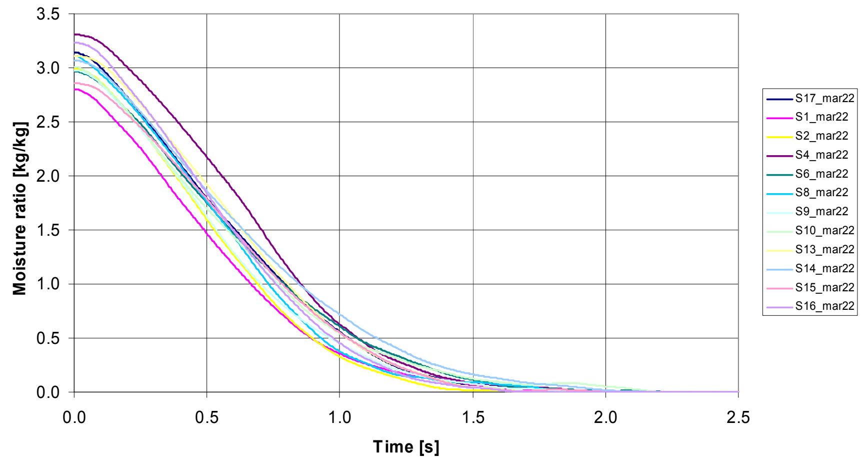

(20 g/m^2, 150 ºC, 1.0 kPa)

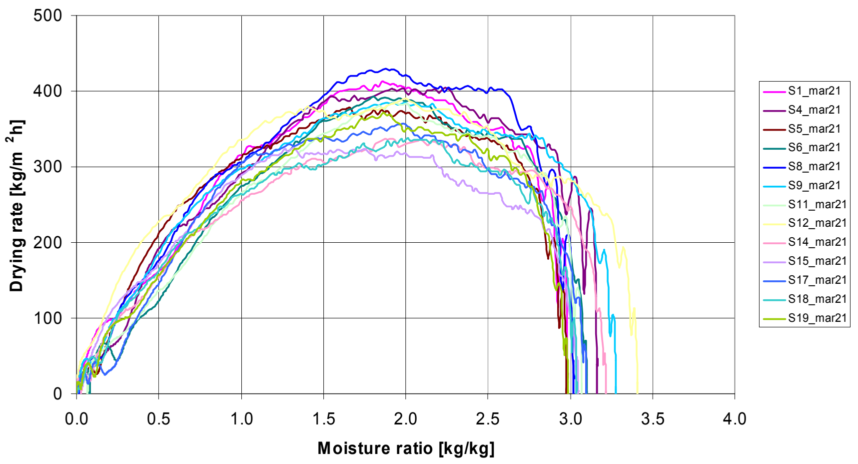

(20 g/m^2, 150 ºC, 1.0 kPa)

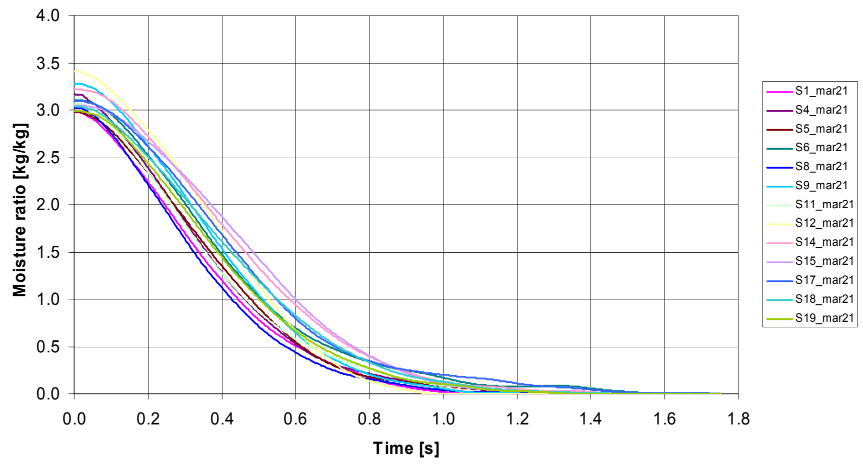

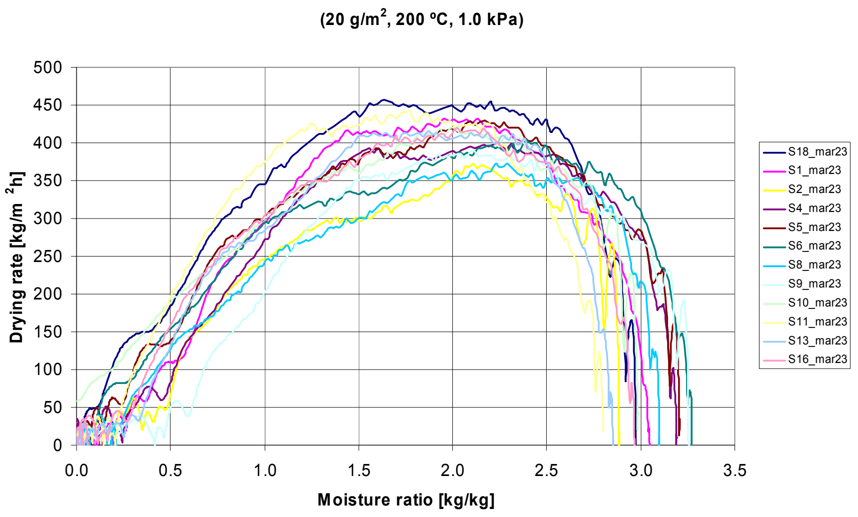
(20 g/m2, 200 ºC, 1.0 kPa)
Drying rate [kg/m 2h]
Moisture ratio [kg/kg]
0
50
100
150
200
250
300
350
400
450
500
0.0
0.5
1.0
1.5
2.0
2.5
3.0
3.5
S18_mar23
S1_mar23
S2_mar23
S4_mar23
S5_mar23
S6_mar23
S8_mar23
S9_mar23
S10_mar23
S11_mar23
S13_mar23
S16_mar23

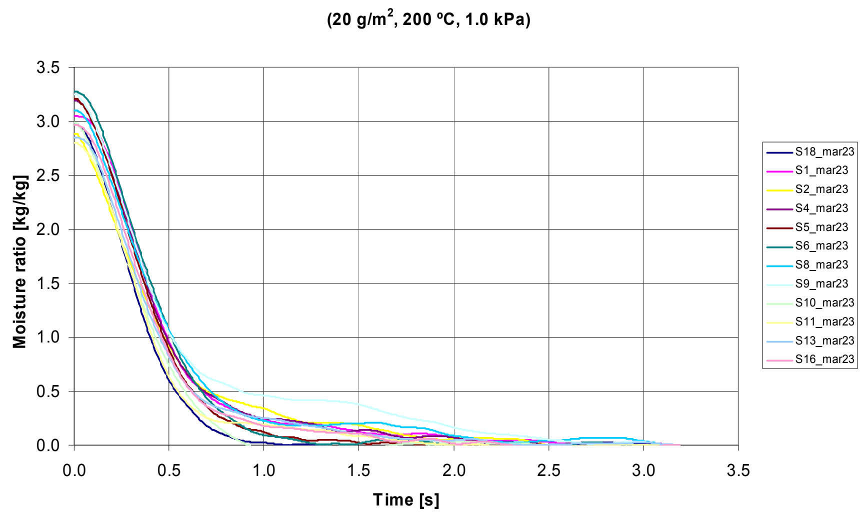
(20 g/m2, 200 ºC, 1.0 kPa)
Moisture ratio [kg/kg]
Time [s]
0.0
0.5
1.0
1.5
2.0
2.5
3.0
3.5
S18_mar23
S1_mar23
S2_mar23
S4_mar23
S5_mar23
S6_mar23
S8_mar23
S9_mar23
S10_mar23
S11_mar23
S13_mar23
S16_mar23

Appendix 3

(20 g/m^2, 100 ºC, 2.7 kPa)

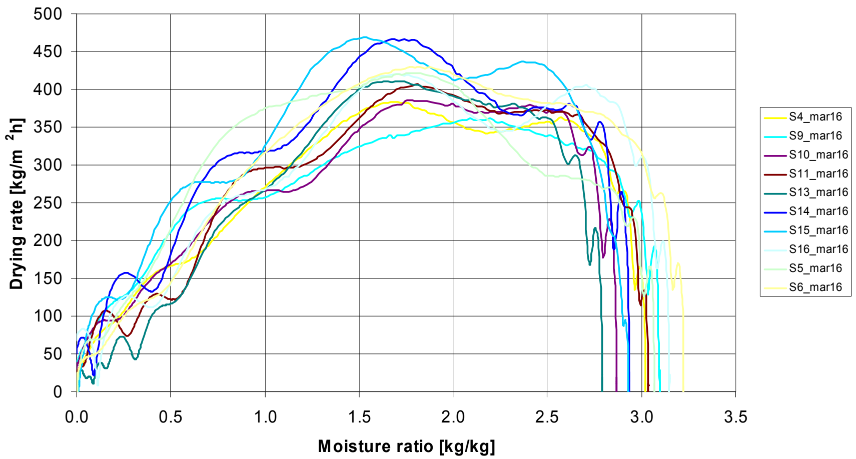

(20 g/m^2, 100 ºC, 2.7 kPa)

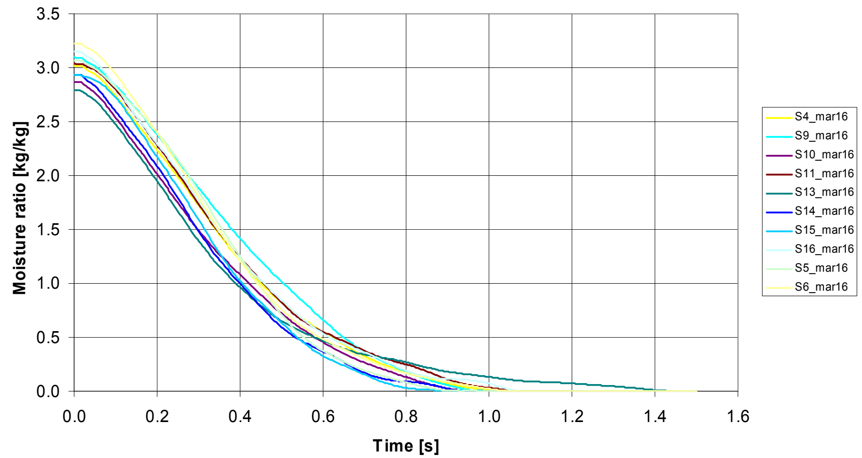

(20 g/m^2, 150 ºC, 2.7 kPa)

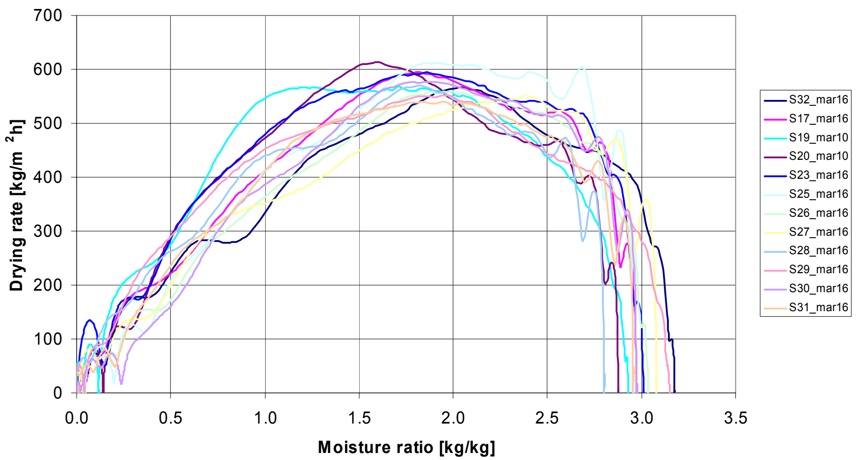

(20 g/m^2, 150 ºC, 2.7 kPa)

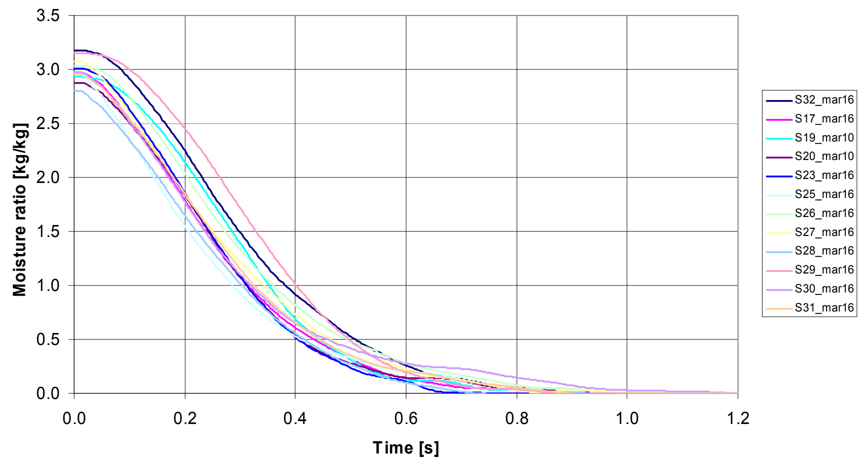

Appendix 3

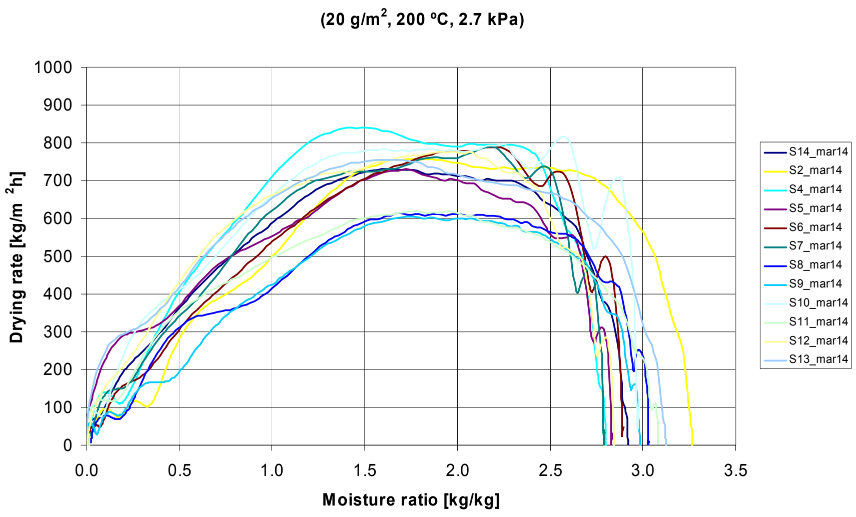
(20 g/m², 200 ºC, 2.7 kPa)
Drying rate [kg/m ²h]
Moisture ratio [kg/kg]
1000
900
800
700
600
500
400
300
200
100
0
0.0
0.5
1.0
1.5
2.0
2.5
3.0
3.5
S14_mar14
S2_mar14
S4_mar14
S5_mar14
S6_mar14
S7_mar14
S8_mar14
S9_mar14
S10_mar14
S11_mar14
S12_mar14
S13_mar14

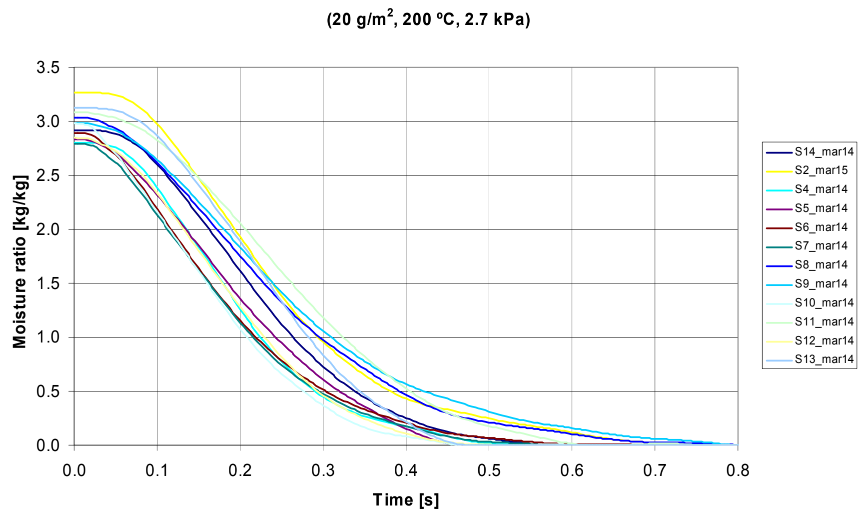
(20 g/m², 200 ºC, 2.7 kPa)
Moisture ratio [kg/kg]
Time [s]
3.5
3.0
2.5
2.0
1.5
1.0
0.5
0.0
0.0
0.1
0.2
0.3
0.4
0.5
0.6
0.7
0.8
S14_mar14
S2_mar15
S4_mar14
S5_mar14
S6_mar14
S7_mar14
S8_mar14
S9_mar14
S10_mar14
S11_mar14
S12_mar14
S13_mar14

Appendix 3

Scheelegatan 3, 212 28 Malmö ● Tel 040-680 07 60 ● Fax 040-680 07 69
www.sgc.se ● info@sgc.se